



INSTITUT
POLYTECHNIQUE
DE PARIS

inria



Hybrid High-Order Methods for the Numerical Simulation of Elasto-Acoustic Wave Propagation

Romain Mottier^{†‡§}

PhD in Applied Mathematics

Advisors: Alexandre Ern^{†‡}, Laurent Guillot[§]

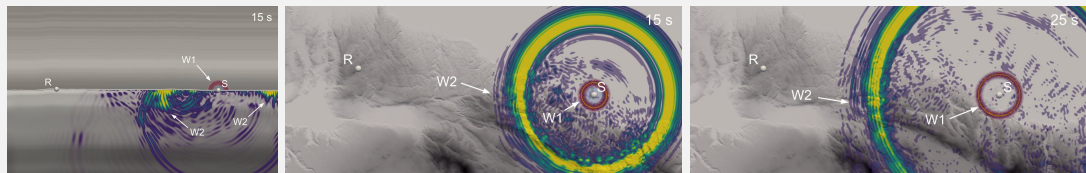
[†] CERMICS, Ecole des Ponts, F-77455 Marne la Vallée cedex 2

[‡] SERENA Project-Team, INRIA Paris, F-75647 Paris France

[§] CEA, DAM, DIF, F-91297 Arpajon, France

Context & motivations

- Mechanical waves: Acoustic (fluid) / Elastic (solid)
- Applications: **Geophysics**, Medical imaging (elastography), Non-destructive testing etc...
- Example: Seismic monitoring of Beyrouth explosion (@Gaël Burgos - CEA/DAM/DASE)



- Objectives: **Detection, Localization, Source characterization**
- **Goal:** Simulate accurately elasto-acoustic waves propagation in **heterogeneous** and **complex** domains

- ▶ System of the form:

$$\mathcal{M}\ddot{\mathbf{U}} + \mathcal{K}\mathbf{U} = \mathbf{F} \quad \text{OR}$$

$$\begin{bmatrix} \mathcal{M}_U & 0 \\ 0 & \mathcal{M}_{\Sigma} \end{bmatrix} \begin{bmatrix} \dot{\mathbf{U}} \\ \dot{\Sigma} \end{bmatrix} + \begin{bmatrix} \mathcal{K}_{UU} & \mathcal{K}_{U\Sigma} \\ \mathcal{K}_{\Sigma U} & \mathcal{K}_{\Sigma\Sigma} \end{bmatrix} \begin{bmatrix} \mathbf{U} \\ \Sigma \end{bmatrix} = \begin{bmatrix} 0 \\ \mathbf{F} \end{bmatrix}$$

- ▶ Discretization: **Hybrid High-Order methods** in space & **Runge–Kutta schemes** in time

Table of Contents

I - State of the art

II - HHO for elasto-acoustic coupling

-  R. Mottier, A. Ern, R. Khot, L. Guillot (2025). Accepted in M2AN
Hybrid high-order methods for elasto-acoustic wave propagation in the time domain
-  R. Mottier, A. Ern, L. Guillot (2025). Submitted to CMAME
Elasto-acoustic wave propagation in geophysical media using hybrid high-order methods on general meshes

III - HHO on unfitted meshes: stabilization by polynomial extension

-  E. Burman, A. Ern, R. Mottier (2025). Submitted to SINUM
Unfitted hybrid high-order methods stabilized by polynomial extension for elliptic interface problems

IV - Conclusion and perspectives

Table of Contents

I - State of the art

- I.1 Numerical methods for wave propagation
- I.2 Hybrid nonconforming methods: HDG/HHO
- I.3 Further insight into HHO

I.1. Numerical methods for wave propagation

- **Finite Differences (FD):** Ideal for simple geometries  [van Vossen, Robertsson, Chapman \(2002\)](#)

- **Finite Element Methods (cG)**  [Marfurt \(1984\)](#)

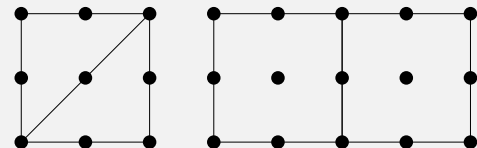
-  [Basabe, Sen \(2007\)](#)

✓ Allow for unstructured meshes

✗ Non-local polynomial bases

✗ Non-diagonal mass matrix:

Mass lumping required for explicit schemes



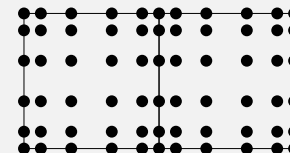
- **Spectral Element Method (SEM)**  [Patera \(1984\)](#)  [Komatitsch, Vilotte \(1998\)](#)  [Cohen \(2002\)](#)

► Quadrature points: tensorized GLL nodes

✓ Diagonal mass matrix

✓ Parallelizable and scalable for HPC applications

✗ Mainly quadrangular/hexahedral meshes



■ Main issue: Complex meshes for realistic geological structures

- ▶ Hard to generate meshes with only one simple shapes
- ▶ Meshes can include hanging nodes (*e.g.* independent subdomains meshing, etc...)

■ Solution: Polytopal discretization methods

QUADRANGLES



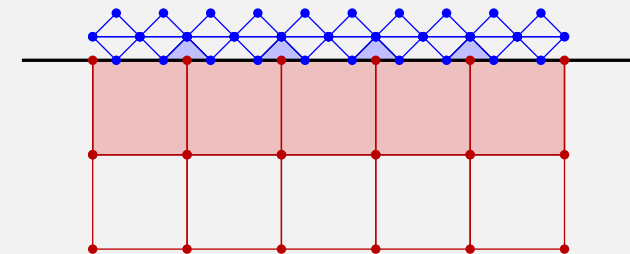
HEXAGONS



TRIANGLES



QUADRANGLES



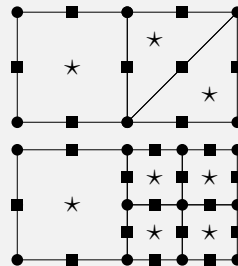
■ Two possibilities:

- ▶ H^1 -conforming polytopal methods: **Virtual Element Methods (VEM)**
- ▶ Nonconforming methods: **class of discontinuous Galerkin methods**

■ Virtual Element Methods (VEM)

- ❑ da Veiga, Brezzi, Cangiani, Manzini, Marini, Russo (2013)
- ❑ Dassi, Fumagalli, Mazzieri, Scotti, Vacca (2022)
- ❑ Wriggers, Junker (2024)

✖ Same issue as cG: **Non-diagonal mass matrix**
 (dofs attached to low-dimensional mesh entities)



■ Discontinuous Galerkin methods (dG)

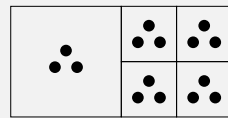
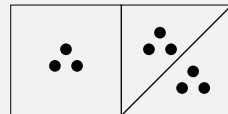
- ❑ Baker (1976) ❑ Wheeler (1978) ❑ Arnold (1982)
- ❑ Grote, Schneebeli, Schötzau (2006)
- ❑ Antonietti, Bonaldi, Mazzieri (2020)

✓ Block-diagonal mass matrix

✖ More dofs than cG

✓ Compact stencil (HPC)

✖ **Stabilization:** Face-based
 (Minimal value)



I.2. Hybrid Nonconforming Methods HDG/HHO

Idea: Additional unknowns attached to mesh faces



Hybridizable discontinuous Galerkin (HDG)

Hybrid High-Order (HHO)

- Seminal papers:
 - Cockburn, Gopalakrishnan, Lazarov (2009)
 - Di Pietro, Ern, Lemaire (2014)
- Wave propagation:
 - Stanglmeier, Nguyen, Peraire, Cockburn (2016)
 - Burman, Duran, Ern, Steins (2021)
 - Kronbichler, Schoeder, Müller, Wall (2016)
 - Burman, Duran, Ern (2022a)
 - Barucq, Rouxelin, Tordeux (2023)
 - Steins, Ern, Jamond, Drui (2023)
- HHO \equiv HDG but with different viewpoints
 - ▶ Approximate $(-\nabla u, u, u|_{\mathcal{F}})$
 - ▶ Approximate $\hat{u} := (u, u|_{\mathcal{F}})$
 - ▶ Gradient is part of unknowns
 - ▶ Explicit gradient reconstruction
 - ▶ Stabilization in numerical flux
 - ▶ Explicit stabilization

HHO \equiv HDG \equiv WG \equiv ncVEM

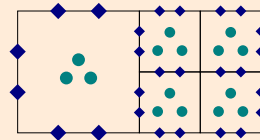
Cockburn, Di Pietro, Ern (2016)

Lemaire (2021)

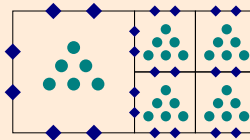
I.3. Further insight into HHO

- Local degrees of freedom:
 - Cell unknowns: $u_T \in P^{k'}(T)$
 - Face unknowns: $u_{\partial T} \in P^k(\partial T)$

EQUAL-ORDER: $k' = k$ ($= 1$)



MIXED-ORDER: $k' = k + 1$ ($= 2$)



● CELL DOFS (DEGREE k')

◆ FACE DOFS (DEGREE k)

Local HHO unknown: $\hat{u}_T := (\textcolor{teal}{u}_T, u_{\partial T}) \in \hat{P}_T^k := P^{k'}(T) \times P^k(\partial T)$

- Global degrees of freedom: $\hat{u}_{\mathcal{M}} := (\textcolor{teal}{u}_{\mathcal{T}}, u_{\mathcal{F}}) \in \hat{P}_{\mathcal{M}}^k := P_{\mathcal{T}}^{k'} \times P_{\mathcal{F}}^k$

► Cell unknowns: $u_{\mathcal{T}} \in P_{\mathcal{T}}^{k'} := \bigtimes_{T \in \mathcal{T}} P^{k'}(T)$

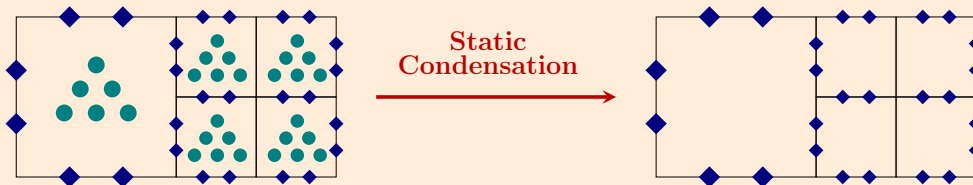
► Face unknowns: $u_{\mathcal{F}} \in P_{\mathcal{F}}^k := \bigtimes_{F \in \mathcal{F}} P^k(F)$

- Algebraic realization for elliptic problem: $(\kappa \nabla u, \nabla w)_\Omega = (f, w)_\Omega$

$$\begin{bmatrix} \mathcal{K}_T & \mathcal{K}_{TF} \\ \mathcal{K}_{FT} & \mathcal{K}_F \end{bmatrix} \begin{bmatrix} U_T \\ U_F \end{bmatrix} = \begin{bmatrix} F_T \\ 0 \end{bmatrix}$$

- Coupling between cell and face unknowns: $\mathcal{K}_F U_F = -\mathcal{K}_{FT} U_T$

- Static condensation: Elimination of cell unknowns



■ Design of local operators

- **Gradient reconstruction** $(\nabla u)|_T \approx \mathbf{g}_T(\hat{u}_T) \in \mathbf{P}^k(T)$: design mimics **integration by parts**

$$\forall \hat{u}_T \in \widehat{P}_T^k \quad (\mathbf{g}_T(\hat{u}_T), \mathbf{q})_T = (\nabla u_T, \mathbf{q})_T - (u_T - u_{\partial T}, \mathbf{q} \cdot \mathbf{n}_T)_{\partial T}, \quad \forall \mathbf{q} \in \mathbf{P}^k(T)$$

- **Stabilization operator:** Weakly enforces matching of trace of cell dofs with face dofs

$$S_{\partial T}(\hat{u}_T) := \begin{cases} \Pi_{\partial T}^k(u_T|_{\partial T} - u_{\partial T}) & \text{mixed-order: Lehrenfeld–Schöberl (HDG)} \\ u_T|_{\partial T} - u_{\partial T} + \text{HOC} & \text{equal-order: High-order correction} \end{cases}$$

■ Same advantages as dG with following improvements:

- ✓ Improved convergence rates: $\|\cdot\|_{H^1}$: $\mathcal{O}(h^{k+1})$ vs. $\mathcal{O}(h^k)$ & $\|\cdot\|_{L^2}$: $\mathcal{O}(h^{k+2})$ vs. $\mathcal{O}(h^{k+1})$
- ✓ Tuning-free and cell-based stabilization
- ✓ Attractive computational costs leveraging static condensation
- ✓ No integration needed on faces for nonlinear problems

Table of Contents

II - Elasto-acoustic coupling

II.1 Model problem

II.2 HHO space semi-discretization

II.3 Runge–Kutta time discretization

II.4 Numerical results



R. Mottier, A. Ern, R. Khot, L. Guillot (2025). Accepted to M2AN

Hybrid high-order methods for elasto-acoustic wave propagation in the time domain



R. Mottier, A. Ern, L. Guillot (2025). Submitted to CMAME

Elasto-acoustic wave propagation in geophysical media using hybrid high-order methods on general meshes

II.1. Model problem

- Wave equations in first-order formulation in time → Wide range of efficient time integrators

- Acoustic wave equation (in Ω^F):

$$\rho^F \partial_t \mathbf{v} - \nabla p = \mathbf{0}$$

$$\frac{1}{\kappa} \partial_t p - \nabla \cdot \mathbf{v} = \mathbf{f}^F$$

Unknowns: p pressure, \mathbf{v} velocity

Parameters: ρ^F , $\kappa \rightarrow c_p^F := \sqrt{\frac{\kappa}{\rho^F}}$

- Elastic wave equation (in Ω^S):

$$\mathbb{C}^{-1}(\lambda, \mu) \partial_t \mathbf{s} - \nabla_{\text{sym}} \mathbf{v} = \mathbf{0}$$

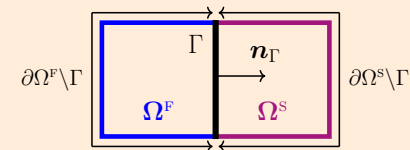
$$\rho^S \partial_t \mathbf{v} - \nabla \cdot \mathbf{s} = \mathbf{f}^S$$

Unknowns: \mathbf{v} velocity, \mathbf{s} stress

Parameters: ρ^S , $\mathbb{C} \rightarrow c_p^S := \sqrt{\frac{\lambda + 2\mu}{\rho^S}}$, $c_s := \sqrt{\frac{\mu}{\rho^S}}$

- Coupling conditions (on $\Gamma = \partial\Omega^F \cap \partial\Omega^S$):

- Kinematic condition: $\mathbf{v} \cdot \mathbf{n}_\Gamma = \mathbf{v} \cdot \mathbf{n}_\Gamma$
- Balance of forces per unit surface: $\mathbf{s} \cdot \mathbf{n}_\Gamma = p \mathbf{n}_\Gamma$



- Initial conditions on (p, \mathbf{v}) and (\mathbf{v}, \mathbf{s})

- Homogeneous Dirichlet boundary conditions on $\partial\Omega$ for simplicity

■ Approximation spaces

$$\begin{aligned} P^F &:= \{p \in H^1(\Omega^F) : p|_{\partial\Omega^F \setminus \Gamma} = 0\}, & M^F &:= L^2(\Omega^F) \\ V^S &:= \{v \in H^1(\Omega^S) : v|_{\partial\Omega^S \setminus \Gamma} = 0\}, & S^S &:= \mathbb{L}_{\text{sym}}^2(\Omega^S) \end{aligned}$$

■ **Weak formulation:** Find $(v, p) : (0, T_f) \rightarrow M^F \times P^F$ and $(s, v) : (0, T_f) \rightarrow S^S \times V^S$ such that, $\forall t \in (0, T_f)$,

► **Acoustic wave equations:** $\forall (r, q) \in M^F \times P^F$,

$$(\partial_t v(t), r)_{\rho^F; \Omega^F} - (\nabla p(t), r)_{\Omega^F} = 0$$

$$(\partial_t p(t), q)_{\frac{1}{\kappa}; \Omega^F} + (v(t), \nabla q)_{\Omega^F} + (v(t) \cdot n_\Gamma, q)_\Gamma = (f^F(t), q)_{\Omega^F}$$

► **Elastic wave equations:** $\forall (b, w) \in S^S \times V^S$,

$$(\partial_t s(t), b)_{\mathbb{C}^{-1}; \Omega^S} - (\nabla_{\text{sym}} v(t), b)_{\Omega^S} = 0,$$

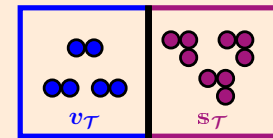
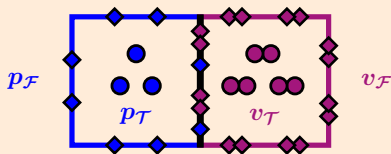
$$(\partial_t v(t), w)_{\rho^S; \Omega^S} + (s(t), \nabla_{\text{sym}} w)_{\Omega^S} - (p(t) n_\Gamma, w)_\Gamma = (f^S(t), w)_{\Omega^S}.$$

► **Skew-symmetry of differential operators**

► **Coupling conditions weakly imposed**

■ Main idea: Primal variables (\mathbf{p} , \mathbf{v}) → HHO discretization & Dual variables (\mathbf{v} , \mathbf{s}) → dG setting

■ Local dofs: HHO: $\hat{\mathbf{p}}_T := (p_T, p_{\partial T}) \in \hat{P}_T^k$, $\hat{\mathbf{v}}_T := (v_T, v_{\partial T}) \in \hat{P}_T^k$ dG: \mathbf{v}_T , \mathbf{s}_T



■ Global dofs: HHO: $\hat{\mathbf{p}}_{\mathcal{M}^F} := (p_{\mathcal{T}^F}, p_{\mathcal{F}^F}) \in \hat{P}_{\mathcal{M}^F}^k$, $\hat{\mathbf{v}}_{\mathcal{M}^S} := (v_{\mathcal{T}^S}, v_{\mathcal{F}^S}) \in \hat{P}_{\mathcal{M}^S}^k$ dG: $\mathbf{v}_{\mathcal{T}^F}$, $\mathbf{s}_{\mathcal{T}^S}$

$$p_{\mathcal{T}^F} \in P_{\mathcal{T}^F}^{k'} := \bigtimes_{T \in \mathcal{T}^F} P^{k'}(T), \quad p_{\mathcal{F}^F} \in P_{\mathcal{F}^F}^k := \bigtimes_{F \in \mathcal{F}^F} P^k(F), \quad \mathbf{v}_{\mathcal{T}^F} \in \mathbf{V}_{\mathcal{T}^F}^k := \bigtimes_{T \in \mathcal{T}^F} \mathbf{P}^k(T)$$

$$\mathbf{v}_{\mathcal{T}^S} \in \mathbf{V}_{\mathcal{T}^S}^{k'} := \bigtimes_{T \in \mathcal{T}^S} \mathbf{P}^{k'}(T), \quad \mathbf{v}_{\mathcal{F}^S} \in \mathbf{V}_{\mathcal{F}^S}^k := \bigtimes_{F \in \mathcal{F}^S} \mathbf{P}^k(F), \quad \mathbf{s}_{\mathcal{T}^S} \in \mathbb{S}_{\mathcal{T}^S}^k := \bigtimes_{T \in \mathcal{T}^S} \mathbb{P}_{\text{sym}}^k(T)$$

II.2. HHO space semi-discretization

- **Acoustic weak formulation (recall):** Find $(\mathbf{v}, p) : (0, T_f) \rightarrow \mathbf{M}^F \times P^F$ such that, $\forall t \in (0, T_f)$,

$$(\partial_t \mathbf{v}(t), \mathbf{r})_{(\rho^F; \Omega^F)} - (\nabla p(t), \mathbf{r})_{\Omega^F} = 0$$

$$(\partial_t p(t), q)_{(\frac{1}{\kappa}; \Omega^F)} + (\mathbf{v}(t), \nabla q)_{\Omega^F} + (\mathbf{v}(t) \cdot \mathbf{n}_\Gamma, q)_\Gamma = (f^F(t), q)_{\Omega^F}$$

- **Acoustic wave equation:** Find $(\hat{p}_{\mathcal{M}^F}, \mathbf{v}_{\mathcal{T}^F}) : (0, T_f) \rightarrow \hat{P}_{\mathcal{M}^F}^k \times \mathbf{V}_{\mathcal{T}^F}^k$ such that, $\forall t \in (0, T_f)$,

$$(\partial_t \mathbf{v}_{\mathcal{T}^F}(t), \mathbf{r}_{\mathcal{T}^F})_{(\rho^F; \Omega^F)} - (\mathbf{g}_{\mathcal{T}^F}(\hat{p}_{\mathcal{M}^F}(t)), \mathbf{r}_{\mathcal{T}^F})_{\Omega^F} = 0$$

$$(\partial_t p_{\mathcal{T}^F}(t), q_{\mathcal{T}^F})_{(\frac{1}{\kappa}; \Omega^F)} + (\mathbf{v}_{\mathcal{T}^F}(t), \mathbf{g}_{\mathcal{T}^F}(\hat{q}_{\mathcal{M}^F}))_{\Omega^F} + s_{\mathcal{M}^F}(\hat{p}_{\mathcal{M}^F}(t), \hat{q}_{\mathcal{M}^F}) + (\mathbf{v}_{\mathcal{F}^S}(t) \cdot \mathbf{n}_\Gamma, q_{\mathcal{F}^F})_\Gamma = (f^F(t), q_{\mathcal{T}^F})_{\Omega^F}$$

- **Elastic wave equation:** Find $(\hat{\mathbf{v}}_{\mathcal{M}^S}, \mathbf{s}_{\mathcal{T}^S}) : (0, T_f) \rightarrow \hat{\mathbf{V}}_{\mathcal{M}^S}^k \times \mathbb{S}_{\mathcal{T}^S}^k$ such that, $\forall t \in (0, T_f)$,

$$(\partial_t \mathbf{s}_{\mathcal{T}^S}(t), \mathbf{b}_{\mathcal{T}^S})_{(\mathbb{C}^{-1}; \Omega^S)} - (\mathbf{g}_{\mathcal{T}^S}^{\text{sym}}(\hat{\mathbf{v}}_{\mathcal{M}^S}(t)), \mathbf{b}_{\mathcal{T}^S})_{\Omega^S} = 0$$

$$(\partial_t \mathbf{v}_{\mathcal{T}^S}(t), \mathbf{w}_{\mathcal{T}^S})_{(\rho^S; \Omega^S)} + (\mathbf{s}_{\mathcal{T}^S}(t), \mathbf{g}_{\mathcal{T}^S}^{\text{sym}}(\hat{\mathbf{w}}_{\mathcal{M}^S}))_{\Omega^S} + s_{\mathcal{M}^S}(\hat{\mathbf{v}}_{\mathcal{M}^S}(t), \hat{\mathbf{w}}_{\mathcal{M}^S}) - (p_{\mathcal{F}^F}(t) \mathbf{n}_\Gamma, \mathbf{w}_{\mathcal{F}^S})_\Gamma = (\mathbf{f}^S(t), \mathbf{w}_{\mathcal{T}^S})_{\Omega^S}$$

- **Stabilizations act only on primal variables**

■ Global stabilization:

- ▶ $s_{\mathcal{M}^F}(\hat{p}_{\mathcal{M}^F}, \hat{q}_{\mathcal{M}^F}) := \sum_{T \in \mathcal{T}^F} \tau_T^F(S_{\partial T}(\hat{p}_T), S_{\partial T}(\hat{q}_T))_{\partial T}$
- ▶ $s_{\mathcal{M}^S}(\hat{\mathbf{v}}_{\mathcal{M}^S}, \hat{\mathbf{w}}_{\mathcal{M}^S}) := \sum_{T \in \mathcal{T}^S} \tau_T^S(\mathbf{S}_{\partial T}(\hat{\mathbf{v}}_T), \mathbf{S}_{\partial T}(\hat{\mathbf{w}}_T))_{\partial T}$

Two strategies:

$$\tau_T^S = \mathcal{O}\left(\frac{1}{h}\right) = \tau_T^F \quad \text{or} \quad \tau_T^S = \mathcal{O}(1) = \tau_T^F$$

(standard for elliptic problem) (standard for hyperbolic problem)

■ Mechanical energy: $\mathcal{E}_h(t) := \frac{1}{2} \|\mathbf{v}_{\mathcal{T}}(t)\|_{\rho^F; \Omega^F}^2 + \frac{1}{2} \|p_{\mathcal{T}}(t)\|_{\frac{1}{\kappa}; \Omega^F}^2 + \frac{1}{2} \|\mathbf{v}_{\mathcal{T}}(t)\|_{\rho^S; \Omega^S}^2 + \frac{1}{2} \|\mathbf{s}_{\mathcal{T}}(t)\|_{\mathbb{C}^{-1}; \Omega^S}^2$

■ Space semi-discrete energy balance

$$\begin{aligned} \mathcal{E}_h(t) + \int_0^t \left\{ s_{\mathcal{M}^F}(\hat{p}_{\mathcal{M}^F}(\tau), \hat{p}_{\mathcal{M}^F}(\tau)) + s_{\mathcal{M}^S}(\hat{\mathbf{v}}_{\mathcal{M}^S}(\tau), \hat{\mathbf{v}}_{\mathcal{M}^S}(\tau)) \right\} d\tau = \\ \mathcal{E}_h(0) + \int_0^t \left\{ (\mathbf{f}^F(\tau), \mathbf{p}_{\mathcal{T}^F}(\tau))_{\Omega^F} + (\mathbf{f}^S(\tau), \mathbf{v}_{\mathcal{T}^S}(\tau))_{\Omega^S} \right\} d\tau \end{aligned}$$

■ Error analysis (under maximal regularity assumption)

$$\begin{aligned} \|\mathbf{v} - \mathbf{v}_{\mathcal{T}^F}\|_{\rho^F; \Omega^F} + \|p - p_{\mathcal{T}^F}\|_{\frac{1}{\kappa}; \Omega^F} &\lesssim \begin{cases} \mathcal{O}(h^{k+\frac{1}{2}}) & \text{for } \mathcal{O}(1)\text{-stabilization} \\ \mathcal{O}(h^{k+1}) & \text{for } \mathcal{O}(\frac{1}{h})\text{-stabilization \& } k' = k + 1 \end{cases} \\ + \|\mathbf{s} - \mathbf{s}_{\mathcal{T}^S}\|_{C^{-1}; \Omega^S} + \|\mathbf{v} - \mathbf{v}_{\mathcal{T}^S}\|_{\rho^S; \Omega^S} \end{aligned}$$

■ Key arguments

- ▶ L^2 -projection for HHO unknowns and HDG⁺-projection for dG unknowns  [Du, Sayas \(2019\)](#)
- ▶ **Error Equations:** Difference between projected exact solution and scheme equations
- ▶ **Stability:** Testing with discrete errors + using classical inequalities
→ discrete energy on lhs and consistency error on rhs
- ▶ **Consistency error bound**

■ Use of the HDG-projection [Cockburn, Gopalakrishnan, Sayas \(2010\)](#)

■ On simplices with $\mathcal{O}(1)$ -stabilization [Ern, Khot \(2024+\):](#)

$$k + \frac{1}{2} \longrightarrow k + 1$$

■ Space semi-discrete algebraic realization

$$\left[\begin{array}{ccc|cc} \mathcal{M}_{\mathcal{T}^F}^{\rho^F} & 0 & 0 & 0 & 0 \\ 0 & \mathcal{M}_{\mathcal{T}^F}^{\frac{1}{\kappa}} & 0 & 0 & 0 \\ 0 & 0 & \mathcal{M}_{\mathcal{T}^S}^{C^{-1}} & 0 & 0 \\ 0 & 0 & 0 & \mathcal{M}_{\mathcal{T}^S}^{\rho^S} & 0 \\ \hline 0 & 0 & 0 & 0 & 0 \\ 0 & 0 & 0 & 0 & 0 \\ 0 & 0 & 0 & 0 & 0 \end{array} \right] \frac{d}{dt} \begin{bmatrix} \mathbf{M}_{\mathcal{T}^F} \\ \mathbf{P}_{\mathcal{T}^F} \\ \mathbf{S}_{\mathcal{T}^S} \\ \mathbf{V}_{\mathcal{T}^S} \\ \hline \mathbf{P}_{\mathcal{F}^F} \\ \mathbf{V}_{\mathcal{F}^S} \end{bmatrix} + \begin{bmatrix} 0 & \mathcal{G}_{\mathcal{T}^F} & 0 & 0 & \mathcal{G}_{\mathcal{T}^F \mathcal{F}^F} & 0 \\ -\mathcal{G}_{\mathcal{T}^F}^\dagger & \Sigma_{\mathcal{T}^F} & 0 & 0 & \Sigma_{\mathcal{T}^F \mathcal{F}^F} & 0 \\ 0 & 0 & 0 & \mathcal{H}_{\mathcal{T}^S} & 0 & \mathcal{H}_{\mathcal{T}^S \mathcal{F}^S} \\ 0 & 0 & -\mathcal{H}_{\mathcal{T}^S}^\dagger & \Sigma_{\mathcal{T}^S} & 0 & \Sigma_{\mathcal{T}^S \mathcal{F}^S} \\ \hline -\mathcal{G}_{\mathcal{T}^F \mathcal{F}^F}^\dagger & \Sigma_{\mathcal{T}^F \mathcal{F}^F}^\dagger & 0 & 0 & \Sigma_{\mathcal{F}^F} & \mathcal{C}_{\mathcal{F}^F} \\ 0 & 0 & -\mathcal{H}_{\mathcal{T}^S \mathcal{F}^S}^\dagger & \Sigma_{\mathcal{T}^S \mathcal{F}^S}^\dagger & -\mathcal{C}_{\mathcal{F}^F}^\dagger & \Sigma_{\mathcal{F}^S} \end{bmatrix} \begin{bmatrix} \mathbf{M}_{\mathcal{T}^F} \\ \mathbf{P}_{\mathcal{T}^F} \\ \mathbf{S}_{\mathcal{T}^S} \\ \mathbf{V}_{\mathcal{T}^S} \\ \hline \mathbf{P}_{\mathcal{F}^F} \\ \mathbf{V}_{\mathcal{F}^S} \end{bmatrix} = \begin{bmatrix} 0 \\ \mathbf{F}_{\mathcal{T}^F} \\ 0 \\ \mathbf{F}_{\mathcal{T}^S} \\ 0 \\ 0 \end{bmatrix}$$

■ Compact formulation:

$$\begin{bmatrix} \mathcal{M}_{\mathcal{T}} & 0 \\ 0 & 0 \end{bmatrix} \frac{d}{dt} \begin{bmatrix} \mathbf{U}_{\mathcal{T}} \\ \mathbf{U}_{\mathcal{F}} \end{bmatrix} + \begin{bmatrix} \mathcal{K}_{\mathcal{T}} & \mathcal{K}_{\mathcal{T} \mathcal{F}} \\ \mathcal{K}_{\mathcal{F} \mathcal{T}} & \mathcal{K}_{\mathcal{F}} \end{bmatrix} \begin{bmatrix} \mathbf{U}_{\mathcal{T}} \\ \mathbf{U}_{\mathcal{F}} \end{bmatrix} = \begin{bmatrix} \mathbf{F}_{\mathcal{T}} \\ 0 \end{bmatrix}$$

- ▶ $\mathcal{K}_{\mathcal{T}}$ is trivially block-diagonal
- ▶ Key question: Is $\mathcal{K}_{\mathcal{F}}$ block-diagonal ? (Important for explicit schemes)

■ Structure of $\mathcal{K}_{\mathcal{F}}$:

$$\mathcal{K}_{\mathcal{F}} = \begin{bmatrix} \Sigma_{\mathcal{F}^F} & \mathcal{C}_{\mathcal{F}^G} \\ -\mathcal{C}_{\mathcal{F}^G} & \Sigma_{\mathcal{F}^S} \end{bmatrix} = \begin{bmatrix} \Sigma_{\mathcal{F}^{OF}} & 0 & 0 & 0 \\ 0 & \Sigma_{\mathcal{F}^{OS}} & 0 & 0 \\ 0 & 0 & \boxed{\begin{matrix} \Sigma_{\mathcal{F}^G} & \mathcal{C}_{\mathcal{F}^G} \\ -\mathcal{C}_{\mathcal{F}^G} & \Sigma_{\mathcal{F}^G} \end{matrix}} \\ 0 & 0 & -\mathcal{C}_{\mathcal{F}^G} & \Sigma_{\mathcal{F}^G} \end{bmatrix} \quad \begin{bmatrix} \Sigma_{F_1^G} & \mathcal{C}_{F_1^G} & 0 & 0 & 0 \\ -\mathcal{C}_{F_1^G} & \Sigma_{F_1^G} & 0 & \vdots & \vdots \\ \vdots & \vdots & 0 & 0 & 0 \\ 0 & 0 & \ddots & 0 & 0 \\ 0 & 0 & 0 & \Sigma_{F_n^G} & \mathcal{C}_{F_1^G} \\ 0 & 0 & 0 & -\mathcal{C}_{F_n^G} & \Sigma_{F_n^G} \end{bmatrix}$$

- $\Sigma_{\mathcal{F}^F}$ and $\Sigma_{\mathcal{F}^S}$ block-diagonal only for **Lehrenfeld–Schöberl** and **Least-squares** stabilizations

$$S_{\partial T}(\hat{p}_T) := \begin{cases} \Pi_{\partial T}^k(p_T|_{\partial T} - p_{\partial T}) & \text{mixed-order: Lehrenfeld–Schöberl (HDG)} \\ p_T|_{\partial T} - p_{\partial T} + \text{H}\times\text{C} & \text{equal-order: Plain Least-squares} \end{cases}$$

- **Coupling terms at interface:** grouping acoustic and elastic dofs of each face

→ $\mathcal{K}_{\mathcal{F}}$ is block diagonal

II.3. Runge–Kutta time discretization

- Recall

$$\begin{bmatrix} \mathcal{M}_T & 0 \\ 0 & 0 \end{bmatrix} \frac{d}{dt} \begin{bmatrix} \mathbf{U}_T \\ \mathbf{U}_{\mathcal{F}} \end{bmatrix} + \begin{bmatrix} \mathcal{K}_T & \mathcal{K}_{T\mathcal{F}} \\ \mathcal{K}_{\mathcal{F}T} & \mathcal{K}_{\mathcal{F}} \end{bmatrix} \begin{bmatrix} \mathbf{U}_T \\ \mathbf{U}_{\mathcal{F}} \end{bmatrix} = \begin{bmatrix} \mathbf{F}_T \\ 0 \end{bmatrix}$$

s-stage Runge–Kutta schemes

SDIRK($s, s+1$) : Truncation order: $\mathcal{O}(\Delta t^{s+1})$

c_1	a_*	0	\cdots	0	
c_2	a_{21}	a_*	\ddots	0	
\vdots	\vdots	\ddots	\ddots	\vdots	
c_s	a_{s1}	\cdots	$a_{s,s-1}$	a_*	
	b_1	\cdots	b_{s-1}	b_s	

ERK(s) : Truncation order: $\mathcal{O}(\Delta t^s)$

c_1	0	\cdots	\cdots	0	
c_2	a_{21}	0	\cdots	0	
\vdots	\vdots	\ddots	\ddots	\vdots	
c_s	a_{s1}	\cdots	$a_{s,s-1}$	0	
	b_1	\cdots	b_{s-1}	b_s	

■ **SDIRK($s, s + 1$) schemes:** For all $i \in \{1, \dots, s\}$,

$$\begin{bmatrix} \mathcal{M}_{\mathcal{T}} & 0 \\ 0 & 0 \end{bmatrix} \begin{bmatrix} \mathbf{U}_{\mathcal{T}}^{n,i} \\ \mathbf{U}_{\mathcal{F}}^{n,i} \end{bmatrix} = \begin{bmatrix} \mathcal{M}_{\mathcal{T}} & 0 \\ 0 & 0 \end{bmatrix} \begin{bmatrix} \mathbf{U}_{\mathcal{T}}^{n-1} \\ \mathbf{U}_{\mathcal{F}}^{n-1} \end{bmatrix} + \Delta t \sum_{j=1}^{\textcolor{red}{i}} a_{ij} \left(\begin{bmatrix} \mathbf{F}_{\mathcal{T}}^{n-1+c_j} \\ 0 \end{bmatrix} - \begin{bmatrix} \mathcal{K}_{\mathcal{T}} & \mathcal{K}_{\mathcal{T}\mathcal{F}} \\ \mathcal{K}_{\mathcal{F}\mathcal{T}} & \mathcal{K}_{\mathcal{F}} \end{bmatrix} \begin{bmatrix} \mathbf{U}_{\mathcal{T}}^{n,j} \\ \mathbf{U}_{\mathcal{F}}^{n,j} \end{bmatrix} \right)$$

► Each stage can be rewritten as

$$\begin{bmatrix} \mathcal{M}_{\mathcal{T}} + a_* \Delta t \mathcal{K}_{\mathcal{T}} & a_* \Delta t \mathcal{K}_{\mathcal{T}\mathcal{F}} \\ a_* \Delta t \mathcal{K}_{\mathcal{F}\mathcal{T}} & a_* \Delta t \mathcal{K}_{\mathcal{F}} \end{bmatrix} \begin{bmatrix} \mathbf{U}_{\mathcal{T}}^{n,i} \\ \mathbf{U}_{\mathcal{F}}^{n,i} \end{bmatrix} = \begin{bmatrix} \mathbf{B}_{\mathcal{T}}^{n,i} \\ \mathbf{B}_{\mathcal{F}}^{n,i} \end{bmatrix}$$

■ **Usual static condensation: Cell dofs elimination**

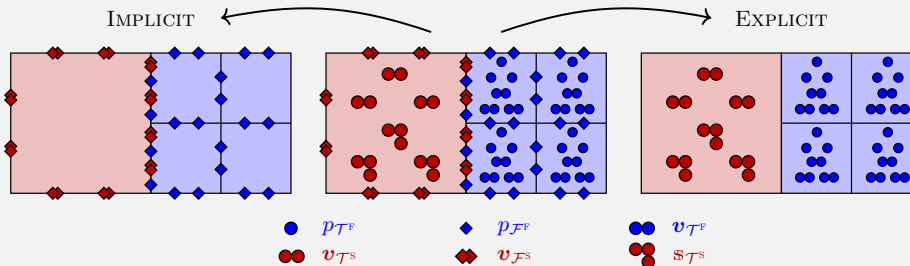
- Global system coupling only face dofs
- Cheap local postprocessing to recover cell dofs

■ **ERK(s) schemes:** For all $i \in \{1, \dots, s\}$,

$$\begin{bmatrix} \mathcal{M}_T & 0 \\ 0 & 0 \end{bmatrix} \begin{bmatrix} U_T^{n,i} \\ U_{\mathcal{F}}^{n,i} \end{bmatrix} = \begin{bmatrix} \mathcal{M}_T & 0 \\ 0 & 0 \end{bmatrix} \begin{bmatrix} U_T^{n-1} \\ U_{\mathcal{F}}^{n-1} \end{bmatrix} + \Delta t \sum_{j=1}^{\textcolor{red}{i-1}} a_{ij} \left(\begin{bmatrix} F_T^{n-1+c_j} \\ 0 \end{bmatrix} - \begin{bmatrix} \mathcal{K}_T & \mathcal{K}_{T\mathcal{F}} \\ \mathcal{K}_{\mathcal{F}T} & \mathcal{K}_{\mathcal{F}} \end{bmatrix} \begin{bmatrix} U_T^{n,j} \\ U_{\mathcal{F}}^{n,j} \end{bmatrix} \right)$$

- ▶ **Face dofs elimination:** $\mathcal{K}_{\mathcal{F}} U_{\mathcal{F}}^{n,j} = -\mathcal{K}_{\mathcal{F}T} U_T^{n,j}$
- ▶ Each stage becomes (**dG rewriting by static condensation**):

$$\mathcal{M}_T U_T^{n,i} = \mathcal{M}_T U_T^{n-1} + \Delta t \sum_{j=1}^{\textcolor{red}{i-1}} a_{ij} \left(F_T^{n-1+c_j} - (\mathcal{K}_T - \mathcal{K}_{T\mathcal{F}} \mathcal{K}_{\mathcal{F}}^{-1} \mathcal{K}_{\mathcal{F}T}) U_T^{n,j} \right)$$



■ Proportion
of face dofs:

		MIXED-ORDER			EQUAL-ORDER			$k \gg 1$
		$k = 1$	$k = 2$	$k = 3$	$k = 1$	$k = 2$	$k = 3$	
2D	ACOUSTIC	20%	17%	15%	25%	20%	17%	$\frac{1}{k}$
	ELASTIC	22%	19%	17%	29%	23%	19%	$\frac{6}{5k}$
3D	ACOUSTIC	21%	19%	17%	27%	23%	20%	$\frac{3}{2k}$
	ELASTIC	25%	23%	21%	33%	29%	25%	$\frac{2}{k}$

→ Elimination of cell dofs much more efficient than face dofs

II.4. Discretization choices

■ Implicit discretization

- ▶ Mixed-order discretization:
 - More unknowns but eliminated by static condensation
 - More efficient than equal-order with specific HHO stabilization
for elliptic problems see  [Cicuttin, Ern, Pignet \(2021\)](#)
- ▶ Lehrenfeld–Schöberl $\mathcal{O}(\frac{1}{h})$ -stabilization
 - Dual unknowns converge at $\mathcal{O}(h^{k+1})$ in L^2 -norm
 - Primal unknowns converge at $\mathcal{O}(h^{k+2})$ in L^2 -norm (**superconvergence numerically observed**)

■ Explicit discretization

- ▶ Equal-order discretization: → Less degrees of freedom
- ▶ Plain Least-Squares stabilization: → Ensure block-diagonal structure
- ▶ $\mathcal{O}(1)$ -stabilization: → Reasonable CFL condition: $\Delta t = \mathcal{O}(h)$

II.5. Numerical results

■ Academic tests cases

- ▶ CFL stability limit
- ▶ Convergences rates

■ Ricker wavelet in bilayered domain

- ▶ Validation by comparison to semi-analytical solution (**Gar6more**)
- ▶ Efficiency: Implicit vs. Explicit

■ Ricker wavelet in sedimentary basin

- ▶ Illustration of HHO mesh flexibility
- ▶ Comparison to a reference solver (**SEM2D**)

■ Creation of a new branch in disk++ library (<https://github.com/wareHHouse/diskpp>)

- ▶ Data structures, Discrete operators, Assembly processes,
Interfacing with various solvers and Preconditioners, and Post-processing

■ Not discussed:

- ▶ Spectral analysis & Study of the energy dissipation
- ▶ Implementation of a 3D spectral HDG method for elastodynamics in HPC code

Academic test case

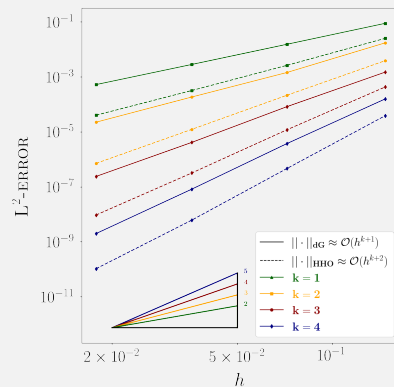
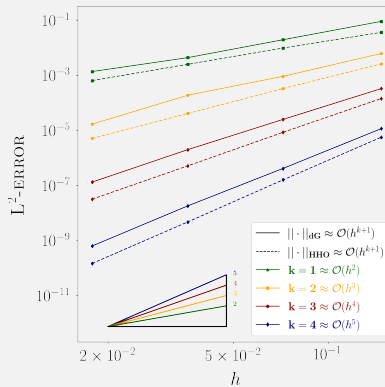
■ Convergence rates on general meshes: recover theoretical rates

Explicit schemes with $\mathcal{O}(1)$ -stabilization:

$$\|\cdot\|_{\text{dG}}: \mathcal{O}(h^{k+1}) \quad \|\cdot\|_{\text{HHO}}: \mathcal{O}(h^{k+1})$$

Implicit schemes with $\mathcal{O}(\frac{1}{h})$ -stabilization:

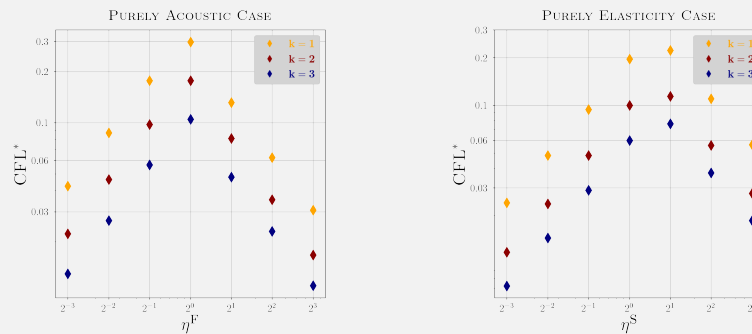
$$\|\cdot\|_{\text{dG}}: \mathcal{O}(h^{k+1}) \quad \|\cdot\|_{\text{HHO}}: \mathcal{O}(h^{k+2})$$



■ Impact of stabilization on CFL stability limit: $c_{\sharp} \frac{\Delta t}{h} \leq \text{CFL}^*(s, k, \eta^f, \eta^s)$

► Weighted $\mathcal{O}(1)$ -stabilization with $\eta^{F/S} := 2^m$ with $m \in [-3, 3]$

$$\tilde{s}_{\mathcal{M}^F}(\hat{p}_{\mathcal{M}^F}, \hat{q}_{\mathcal{M}^F}) := \eta^F s_{\mathcal{M}^F}(\hat{p}_{\mathcal{M}^F}, \hat{q}_{\mathcal{M}^F}), \quad \tilde{s}_{\mathcal{M}^S}(\hat{v}_{\mathcal{M}^S}, \hat{w}_{\mathcal{M}^S}) := \eta^S s_{\mathcal{M}^S}(\hat{v}_{\mathcal{M}^S}, \hat{w}_{\mathcal{M}^S})$$



- Evolution of CFL^* as $\min(\eta, 1/\eta)$ → Optimal CFL for $\eta^F \approx 1 \approx \eta^S$
- $\eta^{f/s} \gg 1 \sim \mathcal{O}(\frac{1}{h})$ -stabilization → degrades CFL

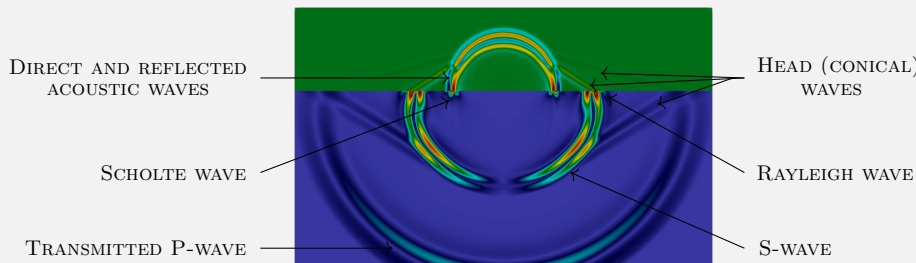
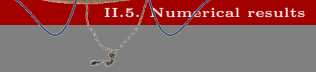
■ Influence of cell geometry

MESHES	$s = 2$			$s = 3$			$s = 4$			
	\triangle	\square	\diamond	\triangle	\square	\diamond	\triangle	\square	\diamond	
$k = 1$	CFL*	0.191	0.205	0.264	0.238	0.253	0.329	0.265	0.282	0.363
	RATIO	1	1.07	1.38	1	1.06	1.38	1	1.06	1.37
$k = 2$	CFL*	0.106	0.099	0.136	0.133	0.123	0.170	0.147	0.138	0.188
	RATIO	1	0.93	1.28	1	0.92	1.28	1	0.94	1.28
$k = 3$	CFL*	0.072	0.063	0.082	0.090	0.079	0.102	0.100	0.087	0.115
	RATIO	1	0.88	1.13	1	0.88	1.13	1	0.87	1.15

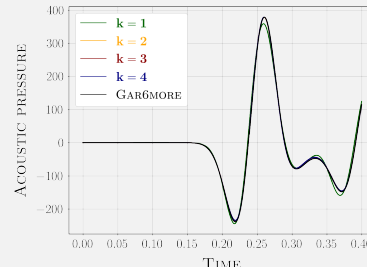
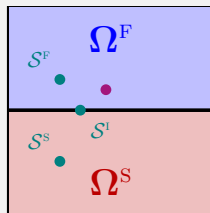
- ▶ CFL* mildly sensitive to mesh geometry
- ▶ CFL improvement for meshes with higher face counts if $k = 1$
- ▶ Less pronounced improvement for $k \geq 2$

Solid subdomain: Hardrock (Granite)

Propagation of a Ricker wavelet in a bilayered domain



■ Comparison to semi-analytical solution (Gar6more) Diaz, Ezziani (2008)



■ Efficiency study: Fair comparison (for 3D perspective)

- ▶ Implicit schemes with **iterative (BiCG) solver** (with ILU preconditioner)
- ▶ Explicit schemes with **time step just below stability limit**

▶ Implicit time steps:
almost 7× larger

▶ Implicit schemes:
decrease by 25%
CPU time

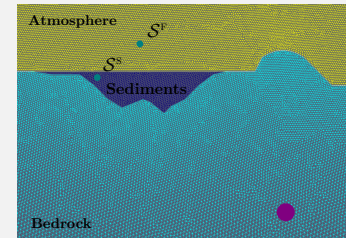
▶ **To be confirmed in 3D**

SCHEMES	SOLVER	CFL*	$\frac{\Delta t}{c_s h}$	RATIO	CPU [s]	RATIO	ERR	
SDIRK(3,4)	$k = 2$ $k = 3$	direct	n/a	0.414	6.90	1125	1	3.15e-02
				0.414	6.90	2284	2.03	2.52e-02
SDIRK(3,4)	$k = 2$ $k = 3$	iterative	n/a	0.414	6.90	2228	1.98	3.91e-02
				0.414	6.90	4216	3.75	3.11e-02
ERK(4)	$k = 2$ $k = 3$	n/a	0.138	0.095	1.36	1533	1.27	2.01e-2
			0.087	0.060	1	5664	5.03	1.90e-2

Propagation of a Ricker wavelet in a sedimentary basin

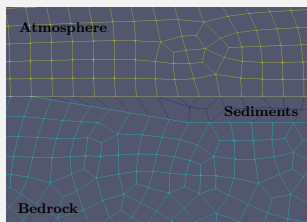
■ Test case setting

MATERIAL	$\rho^F/S \left[\frac{\text{kg}}{\text{m}^3} \right]$	$c_p^F/S \left[\frac{\text{m}}{\text{s}} \right]$	$c_p^S \left[\frac{\text{m}}{\text{s}} \right]$
ATMOSPHERE	1.225	343	n/a
SEDIMENTS	1300	1600	900
BEDROCK	2570	5350	3009

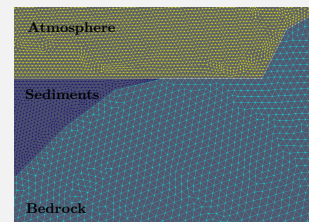


→ Illustration of HHO mesh flexibility: Typical geometry difficult to mesh in 3D

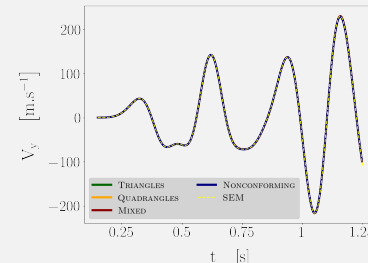
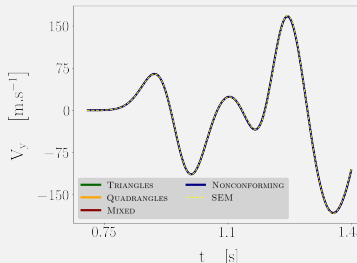
■ Mixed meshes



■ Nonconforming meshes with hanging nodes



■ Comparison with a reference spectral solver



■ Wave trapped into sedimentary basin

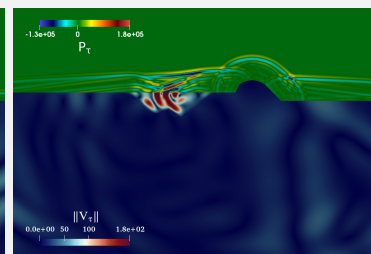
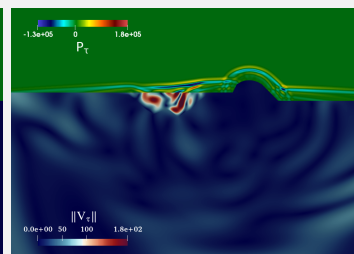
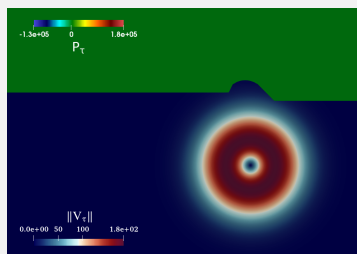


Table of Contents

III - Unfitted HHO stabilized by polynomial extension

II.1 Motivation & model problem

II.2 Unfitted FEM

II.3 Unfitted HHO

II.4 Polynomial extension

II.5 Numerical results



E. Burman, A. Ern, R. Mottier (2025). Submitted to SINUM

*Unfitted hybrid high-order methods stabilized by polynomial
extension for elliptic interface problems*

III.1. Motivation & model problem

- **Goal:** Accurate simulation of elasto-acoustic waves in **heterogeneous domains with complex geometries**
- **HHO methods:** ✓ Allow for efficient implicit and explicit time discretizations
✓ Work on general meshes
✗ Polytopal methods work optimally on planar faces

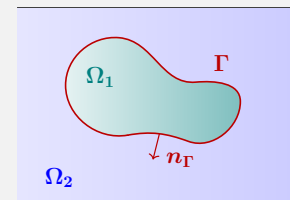
▲ What if interfaces cannot be meshed with planar faces

Idea: Use of unfitted HHO methods to handle curved interfaces

■ First step towards wave equation: Elliptic interface problem

► Strong form:

$$\begin{cases} -\nabla \cdot (\kappa \nabla p) = f & \text{in } \Omega_1 \cup \Omega_2 \\ \llbracket p \rrbracket_{\Gamma} = g_D & \text{on } \Gamma \\ \llbracket \kappa \nabla p \rrbracket_{\Gamma} \cdot \mathbf{n}_{\Gamma} = g_N & \text{on } \Gamma \\ p = 0 & \text{on } \partial\Omega \end{cases}$$

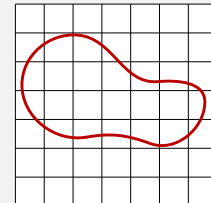


► Weak form: Find $p \in H^1(\Omega_1 \cup \Omega_2)$, such that $\llbracket p \rrbracket_{\Gamma} = g_D$ and $\mathbf{a}(p, q) = \ell(q)$ with

- $\mathbf{a}(p, q) := \sum_{i \in \{1, 2\}} (\kappa \nabla p_i, \nabla q_i)_{\Omega_i}$
- $\ell(q) := (f, q)_{\Omega} + (g_N, q)_{\Gamma}$

III.2. Unfitted FEM: Basic concepts

- Main idea: Minimize complexity of mesh generation
 - ▶ Mesh cells arbitrarily cut by physical interfaces



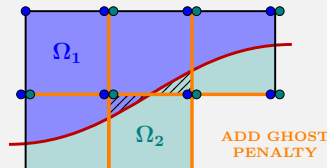
■ Unfitted FEM

- ▶ Handle cut cells by doubling unknowns: (maintain optimality)

[Hansbo, Hansbo \(2002\)](#)

- ▶ Ill-cut cell stabilization: Ghost penalty

[Burman \(2010\)](#)

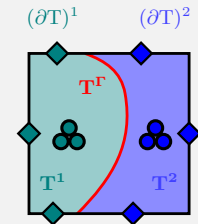


III.3. Unfitted HHO

- Seminal papers: Burman, Ern (2018) Burman, Cicuttin, Delay, Ern (2021)
- Different applications: Stokes interface problems Burman, Delay, Ern (2021)
Wave propagation (second-order form) Burman, Duran, Ern (2022b)

■ Doubling cell and face unknowns in cut cells:

$$\hat{p}_T := (\hat{p}_{T^1}, \hat{p}_{T^2}) := (p_{T^1}, p_{(\partial T)^1}, p_{T^2}, p_{(\partial T)^2}) \in \hat{P}_T^k := \hat{P}_{T^1}^k \times \hat{P}_{T^2}^k$$

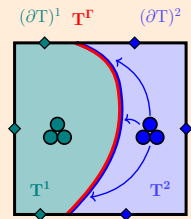


- No unknown attached to interface
 - ▶ Need of mixed-order discretization: $k' = k + 1$

■ Notation: $T^i := T \cap \Omega^i$, $(\partial T)^i := \partial T \cap \Omega^i$, $T^\Gamma := \partial T \cap \Gamma$

■ Gradient reconstruction

- ▶ Gradient is reconstructed in each sub-cell
- ▶ Jump across interface is accounted for in gradient reconstruction and close integration by parts



$$(\mathbf{g}_{T^i}(\hat{p}_T), \mathbf{q})_{T^i} := (\nabla p_{T^i}, \mathbf{q})_{T^i} + (p_{(\partial T)^i} - p_{T^i}, \mathbf{q} \cdot \mathbf{n}_T)_{(\partial T)^i} - \delta_{i1}([\![p_T]\!]_\Gamma, \mathbf{q} \cdot \mathbf{n}_\Gamma)_{T^\Gamma}$$

- ▶ Robustness wrt contrast $\kappa_1 \ll \kappa_2$: non-symmetric inclusion of $[\![p_T]\!]_\Gamma$

■ Stabilization

- Usual mixed-order LS $\mathcal{O}(\frac{1}{h})$ -stabilization (on internal faces):

$$s_{\mathcal{M}}^{\circ}(\hat{p}_{\mathcal{M}}, \hat{q}_{\mathcal{M}}) := \sum_{T \in \mathcal{T}} \sum_{i \in \{1,2\}} \frac{\kappa_i}{h_T} (\Pi_{(\partial T)^i}^k (p_{T^i} - p_{(\partial T)^i}), q_{T^i} - q_{(\partial T)^i})_{(\partial T)^i}$$

- Nitsche-like penalty (at interfaces):

$$s_{\mathcal{M}}^{\Gamma}(\hat{p}_{\mathcal{M}}, \hat{q}_{\mathcal{M}}) := \sum_{T \in \mathcal{T}} \delta_{i1} \frac{\kappa_1}{h_T} ([\![p_T]\!], [\![q_T]\!])_{T^\Gamma}$$

- Total stabilization:

$$s_{\mathcal{M}}(\hat{p}_{\mathcal{M}}, \hat{q}_{\mathcal{M}}) := s_{\mathcal{M}}^{\circ}(\hat{p}_{\mathcal{M}}, \hat{q}_{\mathcal{M}}) + s_{\mathcal{M}}^{\Gamma}(\hat{p}_{\mathcal{M}}, \hat{q}_{\mathcal{M}})$$

■ Discrete problem: $a_{\mathcal{M}}(\hat{p}_{\mathcal{M}}, \hat{q}_{\mathcal{M}}) := \ell_{\mathcal{M}}(\hat{q}_{\mathcal{M}})$

► Discrete bilinear form:

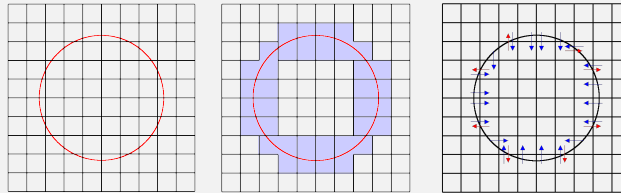
$$a_{\mathcal{M}}(\hat{p}_{\mathcal{M}}, \hat{q}_{\mathcal{M}}) := \sum_{T \in \mathcal{T}} \sum_{i \in \{1,2\}} \kappa_i(\mathbf{g}_{T^i}(\hat{p}_{\mathcal{M}}), \mathbf{g}_{T^i}(\hat{q}_{\mathcal{M}}))_{T^i} + s_{\mathcal{M}}(\hat{p}_{\mathcal{M}}, \hat{q}_{\mathcal{M}})$$

► Discrete linear form (with $\ell_{\mathcal{M}}$ defined so as to ensure consistency):

$$\ell_{\mathcal{M}}(\hat{q}_{\mathcal{M}}) := \sum_{T \in \mathcal{T}} \sum_{i \in \{1,2\}} (f, w_{T^i})_{T^i} + \sum_{T \in \mathcal{T}^{\text{cut}}} (g_N, q_{T^2})_{T^{\Gamma}} + \sum_{T \in \mathcal{T}^{\text{cut}}} \kappa_1(g_D, [\![q_T]\!] h_T^{-1} - \mathbf{g}_{T^1} \cdot \mathbf{n}_{\Gamma})_{T^{\Gamma}}$$

■ Unfitted HHO method: handling of curved interfaces in well-cut configuration
 → Need to stabilize ill-cut configurations

Stabilization of ill-cut cells



■ Cell agglomeration: Sollie, Bokhove, van der Vegt (2011) Johansson, Larson (2013)

- ✓ Leverages on polyhedral capacity of HHO methods → **No change in numerical scheme**
- ✗ **Intrusive on mesh data structure**

■ Polynomial extension: This Thesis

- ✓ Works on initial mesh (non-intrusive on mesh data structure)
- ✗ Requires modification of stencil: **intrusive at assembly level**

■ Common feature: **Pairing operator**

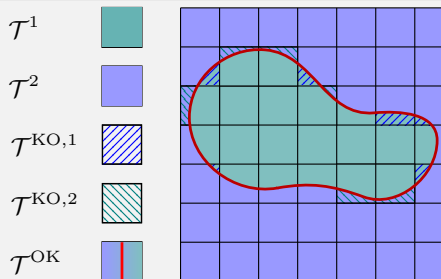
■ Mesh partitioning

$$\mathcal{T} := \mathcal{T}^{\text{uncut}} \cup \mathcal{T}^{\text{cut}}$$

$$\mathcal{T}^{\text{cut}} := \mathcal{T}^{\text{OK}} \cup \mathcal{T}^{\text{KO}} := \mathcal{T}^{\text{OK}} \cup \mathcal{T}^{\text{KO},1} \cup \mathcal{T}^{\text{KO},2}$$

■ Ball condition

- ▶ For a fixed parameter $\vartheta \in (0, 1)$: $T \in \mathcal{T}^{\text{OK}} \Rightarrow T^i$ contain a ball of radius $\vartheta h_T \quad \forall i \in \{1, 2\}$
- ▶ $\mathcal{T}^{\text{KO},1} \cap \mathcal{T}^{\text{KO},2} = \emptyset$ if mesh fine enough  Burman, Ern (2018)

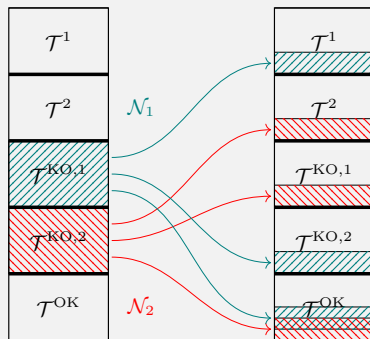


■ Pairing operator:

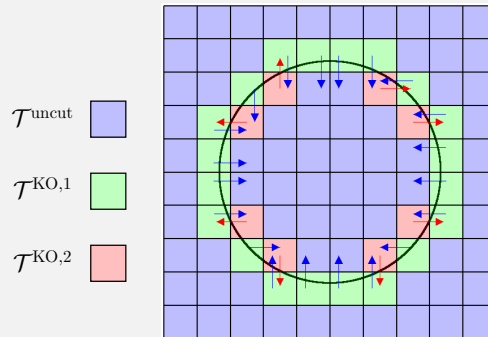
$$\mathcal{N}_i : \mathcal{T}^{\text{KO},i} \ni S \longmapsto T \in (\mathcal{T}^i \cup \mathcal{T}^{\text{OK}} \cup \mathcal{T}^{\text{KO},\bar{i}}) \cap \Delta_1(S), \quad \forall i \in \{1, 2\}$$

- $\Delta_1(S)$: first layer of neighboring cells of S

Pairing operator



Example



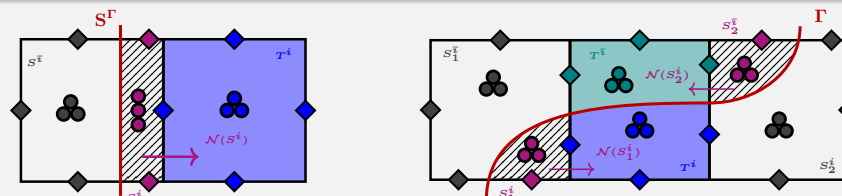
III.4. Polynomial extension

■ Main idea:

- ▶ Enlarge stencil: $\hat{p}_T^{\mathcal{N}} := (\hat{p}_T, (\hat{p}_S)_{S \in \mathcal{N}^{-1}(T)}) \in \hat{P}_T^{\mathcal{N}} := \hat{P}_T^k \times \bigtimes_{S \in \mathcal{N}^{-1}(T)} \hat{P}_S^k$
- ▶ Use ill-cut cells dofs in gradient reconstruction of well-cut and uncut (sub)cells
- ▶ Stabilize ill-cut cells dofs

■ Local gradient reconstruction: If subcell T^i satisfies ball condition

$$\begin{aligned}
 (\mathbf{g}_{T^i}(\hat{p}_T^{\mathcal{N}}), \mathbf{q})_{T^i} &:= (\nabla p_{T^i}, \mathbf{q})_{T^i} + (p_{(\partial T)^i} - p_{T^i}, \mathbf{q} \cdot \mathbf{n}_T)_{(\partial T)^i} - \delta_{i1}([\![p_T]\!]_{\Gamma}, \mathbf{q} \cdot \mathbf{n}_{\Gamma})_{T^{\Gamma}} \\
 &\quad + \sum_{S \in \mathcal{N}_i^{-1}(T)} \left\{ (p_{(\partial S)^i} - p_{S^i}, \mathbf{q}^+ \cdot \mathbf{n}_S)_{(\partial S)^i} - \delta_{i1}([\![p_S]\!]_{\Gamma}, \mathbf{q}^+ \cdot \mathbf{n}_{\Gamma})_{S^{\Gamma}} \right\}
 \end{aligned}$$



■ **Stabilization:** Lehrenfeld–Schöberl stabilization & Nitsche-like penalty at interface

- ▶ Ill-cut stabilization: Direct ghost penalty on skeleton

 Preuß (2018)  Lehrenfeld, Olshanskii (2019)

$$s_{\mathcal{M}}^{\mathcal{N}}(\hat{p}_{\mathcal{M}}, \hat{q}_{\mathcal{M}}) := \sum_{(T,i) \in \mathcal{P}_h^{\text{OK}}} \sum_{S \in \mathcal{N}_i^{-1}(T)} \frac{\kappa_i}{h_S} (\underline{p}_{S^i} - p_{T^i}^+, \underline{q}_{S^i} - q_{T^i}^+)_{S^i}$$

- Connect ill-cut cell dofs with well-cut or uncut cell dofs

■ **Main error estimate:** Let $p \in H^s(\Omega_1 \cup \Omega_2)$ with $s \in (\frac{3}{2}, k+2]$

$$\left\{ \sum_{T \in \mathcal{T}} \sum_{i \in \{1,2\}} \kappa_i \|\nabla(p_i - p_{T^i})\|_{T^i}^2 \right\}^{\frac{1}{2}} \lesssim h^{s-1} \sum_{i \in \{1,2\}} \kappa_i^{\frac{1}{2}} |p_i|_{H^s(\Omega_i)}$$

- ▶ Optimal convergence rates in H^1 -norm: $O(h^{k+1})$

III.5. Implementation details

- New branch in ProtoN C++ library with following features (**porting to disk++ in progress**)

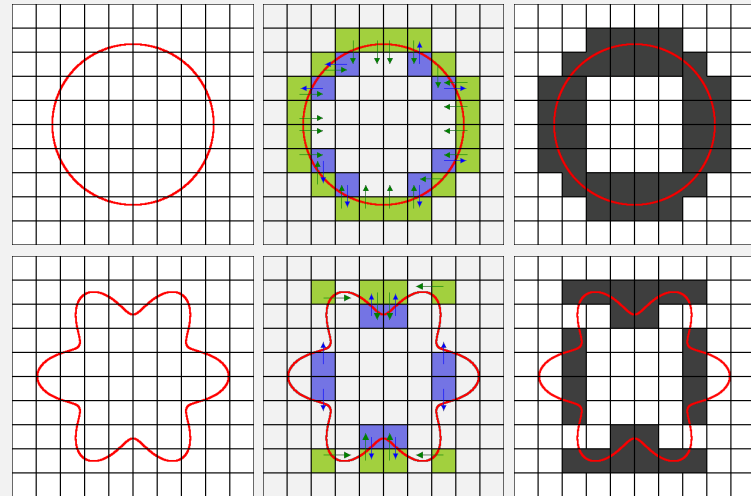
- ▶ Modal (centered and scaled) bases attached to sub-cells
- ▶ Quadratures in cut cells based on **sub-triangulation**, using a pcw. linear approximation of interface into 2^r ($r \approx 6$) **segments**

- Improvement of polynomial integration in cut cells

- ▶ Isoparametric description of interface  [Lehrenfeld \(2016\)](#)
- ▶ Successive integration by parts  [Antonietti, Houston, Pennesi \(2018\)](#)

III.6. Numerical results

$T \in \mathcal{T}^{\text{KO},1}$



$T \in \mathcal{T}^{\text{KO},2}$



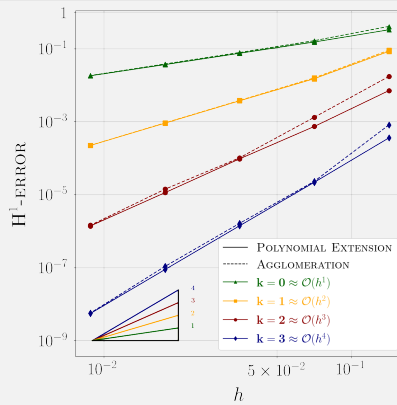
AGGLOMERATED
CELL



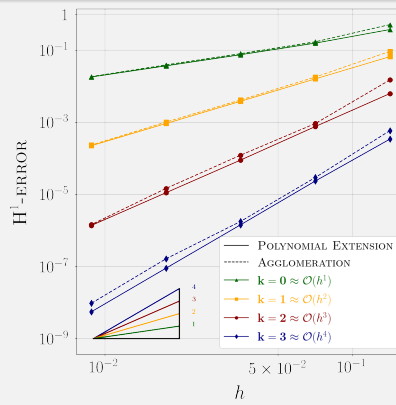
Convergence rates on smooth solutions

$$u(x, y) = \sin(\pi x) \sin(\pi y), \quad g_D = g_N = 0, \quad \kappa_1 = \kappa_2 = 1$$

Circular interface

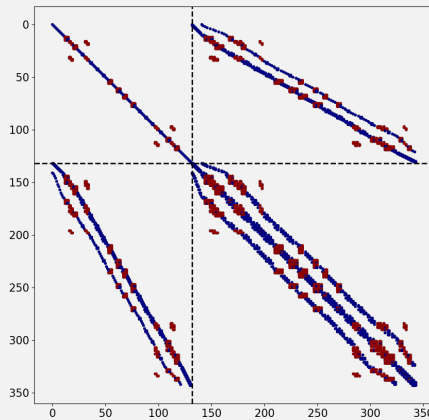


Flower-like interface

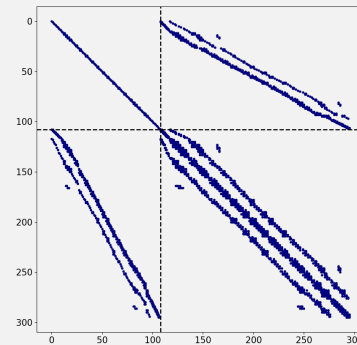


Comparison of matrix sparsity profiles

Polynomial extension



Cell agglomeration

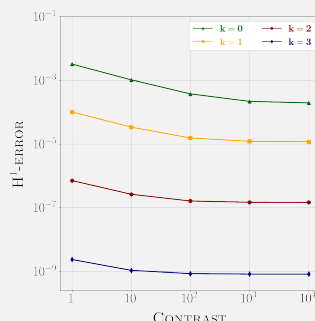


Solutions with contrasted diffusivity

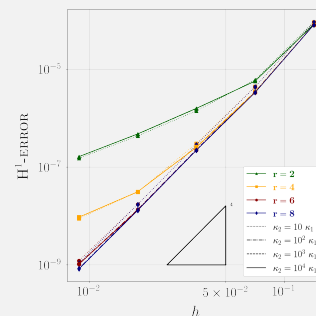
- Circular interface, no jumps ($g_D = g_N = 0$), polar coordinates (ρ, θ) :

$$u_1(\rho) = \frac{\rho^6}{\kappa_1}, \quad u_2(\rho) = \frac{\rho^6}{\kappa_2} + R^6 \left(\frac{1}{\kappa_1} - \frac{1}{\kappa_2} \right)$$

- H^1 -Error vs. $\kappa_2 = 10^m \kappa_1$, $r = 10$



- H^1 -Error vs. h , $k = 3$, $r \in \{2, 4, 6, 8\}$:



- Robustness wrt contrast

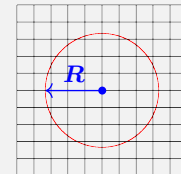
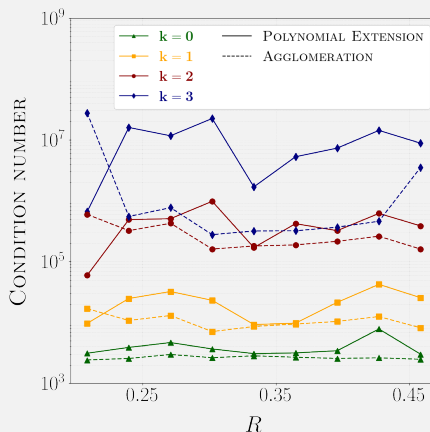
- Same conclusions for non-polynomial jumps

- High quality quadrature in subcell

Conditioning of stiffness matrix

- Circular interface with radius:

$$R = \frac{1}{3} + \frac{i}{32}, \quad i \in \{-4, \dots, 4\}$$



- Grow of conditioning with polynomial degree
- Robust conditioning for circular interface

Conclusion

Summary

- **HHO:** Accurate and robust simulation of elasto-acoustic wave propagation
 - ▶ Efficient implicit and explicit time discretizations
 - ▶ Allows for **general meshes**
- **unfitted HHO** for elliptic interface problem
 - ▶ Novel stabilization with **polynomial extension**

Perspectives

- Radiative boundary conditions: Robin, PML etc...  [Berenger \(1994\)](#)
- Extension to other physics: linear attenuation, anisotropy, poroelasticity, etc...
- Structure-preserving RK schemes (symplectic or energy-preserving)
 [Sánchez, Cockburn, Nguyen, Peraire \(2021\)](#)
- **unfitted HHO** for elasto-acoustic wave propagation
- **SEM-HHO coupling**

**THANK YOU FOR YOUR
ATTENTION!**

Error estimate coupling wave problem

■ Focus on acoustic subdomain

- (1) **Error equations:** For all $t \in \bar{J}$,

$$\begin{aligned}\mathbf{N}_{\mathcal{T}^F}(t) &:= \mathbf{v}_{\mathcal{T}^F}(t) - \mathbf{I}_{\mathcal{T}^F}^{H+}(\mathbf{v}(t)) \\ \hat{e}_{\mathcal{M}^F}(t) &:= \hat{p}_{\mathcal{M}^F}(t) - \hat{I}_{\mathcal{M}^F}^{HHO}(p(t))\end{aligned}$$

- ▶ **Error on dual variable:** For all $\mathbf{r}_{\mathcal{T}^F} \in \mathcal{V}_{\mathcal{T}^F}^k$,

$$(\partial_t \mathbf{N}_{\mathcal{T}^F}(t), \mathbf{r}_{\mathcal{T}^F})_{\rho^F; \Omega^F} - (\mathbf{G}_{\mathcal{T}^F}(\hat{e}_{\mathcal{M}^F}(t)), \mathbf{r}_{\mathcal{T}^F})_{\Omega^F} = (\partial_t \mathbf{v}(t) - \mathbf{I}_{\mathcal{T}^F}^{H+}(\partial_t \mathbf{v}(t)), \mathbf{r}_{\mathcal{T}^F})_{\rho^F; \Omega^F}$$

- ▶ **Error on primal variable:** For all $\hat{q}_{\mathcal{M}^F} \in \hat{\mathcal{U}}_h^F$,

$$\begin{aligned}(\partial_t e_{\mathcal{T}^F}(t), q_{\mathcal{T}^F})_{\frac{1}{\kappa}; \Omega^F} + (\mathbf{N}_{\mathcal{T}^F}(t), \mathbf{G}_{\mathcal{T}^F}(\hat{q}_{\mathcal{M}^F}))_{L^2(\Omega^F)} + s_{\mathcal{M}^F}(\hat{e}_{\mathcal{M}^F}(t), \hat{q}_{\mathcal{M}^F}) + (\mathbf{e}_{\mathcal{F}^S}(t) \cdot \mathbf{n}_\Gamma, q_{\mathcal{F}^F})_\Gamma \\ = \sum_{T \in \mathcal{T}^F} ((\mathbf{v}(t) - \mathbf{I}_T^{H+}(\mathbf{v}(t))) \cdot \mathbf{n}_T, \Pi_{\partial T}^k(q_{\partial T} - q_T))_{\partial T} - s_{\mathcal{M}^F}(\hat{I}_{\mathcal{M}^F}^{HHO}(p(t)), \hat{q}_{\mathcal{M}^F})\end{aligned}$$

Error estimate coupling wave problem

- (2) **Stability:** Testing with discrete errors, for all $t \in \overline{J}$,

$$\begin{aligned} & \frac{1}{2} \frac{d}{dt} \left\{ \|e_{\mathcal{T}^F}(t)\|_{\frac{1}{\kappa}; \Omega^F}^2 + \|\mathbf{N}_{\mathcal{T}^F}(t)\|_{\rho^F; \Omega^F}^2 + \dots \right\} + s_{\mathcal{M}^F}(\hat{e}_{\mathcal{M}^F}(t), \hat{e}_{\mathcal{M}^F}(t)) + \dots \\ & = (\partial_t \mathbf{m}(t) - \mathbf{I}_{\mathcal{T}^F}^{H+}(\partial_t \mathbf{m}(t)), \mathbf{N}_{\mathcal{T}^F}(t))_{\rho^F; \Omega^F} + \dots + \psi_{\mathcal{M}^F}((\mathbf{m}(t), p(t)); \hat{e}_{\mathcal{M}^F}(t)) + \dots \end{aligned}$$

- ▶ **Acoustic consistency error:**

$$\begin{aligned} \psi_{\mathcal{M}^F}((\mathbf{m}(t), p(t)); \hat{q}_{\mathcal{M}^F}) &:= \sum_{T \in \mathcal{T}^F} ((\mathbf{m}(t) - \mathbf{I}_T^{H+}(\mathbf{m}(t))) \cdot \mathbf{n}_T, \Pi_{\partial T}^k(q_{\partial T} - q_T))_{L^2(\partial T)} \\ &\quad - s_{\mathcal{M}^F}(\hat{I}_{\mathcal{M}^F}^{HHO}(p(t)), \hat{q}_{\mathcal{M}^F}) \end{aligned}$$

Spectral analysis

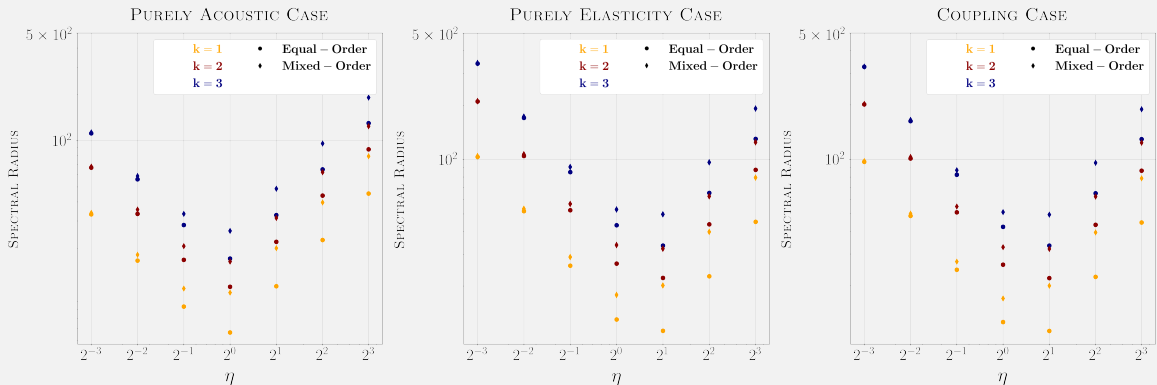


Figure 1: Spectral radius in the equal-Order and mixed-Order settings for the pure acoustic, pure linear elasticity, and elasto-acoustic coupling cases with $k \in \{1:3\}$

	$k \backslash \eta/\eta_*$	1/8	1/4	1/2	1	2	4	8
	k	1	2	3	4	5	6	7
EQUAL-ORDER	1	55.3	27.8	14.2	9.9	19.7	39.5	78.9
	2	114.8	57.8	29.5	19.5	38.3	76.3	152.5
	3	185.2	93.2	47.7	29.6	57.3	113.9	227.3
MIXED-ORDER	1	94.2	48.3	26.3	16.5	20.7	41.0	81.7
	2	195.0	99.3	53.0	31.8	33.2	64.7	128.7
	3	314.3	159.6	84.3	50.0	51.3	99.4	197.4

Table 1: Spectral radius in the equal- and mixed-order settings for the elasto-acoustic coupling with reference weights and $k \in \{1:3\}$

	SIMPLICIAL MESHES \triangle		QUADRAGULAR MESHES \square		POLYGONAL MESHES \diamond	
	EQUAL-ORDER	MIXED-ORDER	EQUAL-ORDER	MIXED-ORDER	EQUAL-ORDER	MIXED-ORDER
$k = 1$	11.6	17.6	9.9	16.5	10.5	20.1
$k = 2$	21.3	31.4	19.5	31.8	20.7	37.2
$k = 3$	33.4	47.8	29.6	50.0	35.2	59.4
$k = 4$	49.2	69.5	45.3	74.0	53.9	86.6
$k = 5$	68.0	93.7	61.5	100.6	76.6	118.9
$k = 6$	90.1	123.2	83.0	134.0	103.5	156.3

Table 2: Spectral radius for different cell geometries in equal- and mixed-order settings with $k \in \{1:6\}$ and optimal setting for η^F and η^S

Butcher tables of RK schemes

$$\begin{array}{c|cc}
 \frac{1}{4} & \frac{1}{4} & 0 \\
 \frac{3}{4} & \frac{1}{2} & \frac{1}{4} \\ \hline
 & \frac{1}{2} & \frac{1}{2}
 \end{array}
 \quad
 \begin{array}{c|ccc}
 \theta & \theta & 0 & 0 \\
 \frac{1}{2} & \frac{1}{2} - \theta & \theta & 0 \\
 1 - \theta & 2\theta & 1 - 4\theta & \theta \\ \hline
 & \xi & 1 - 2\xi & \xi
 \end{array} \tag{1a}$$

SDIRK(3,4) scheme corresponds to the values $\theta := \frac{1}{\sqrt{3}} \cos\left(\frac{\pi}{18}\right) + \frac{1}{2}$ and $\xi := \frac{1}{6(2\theta-1)^2}$

$$\begin{array}{c|cc}
 0 & 0 & 0 \\
 \frac{1}{2} & \frac{1}{2} & 0 \\ \hline
 & 0 & 1
 \end{array}
 \quad
 \begin{array}{c|ccc}
 0 & 0 & 0 & 0 \\
 \frac{1}{2} & \frac{1}{2} & 0 & 0 \\
 1 & -1 & 2 & 0 \\ \hline
 & \frac{1}{6} & \frac{2}{3} & \frac{1}{6}
 \end{array}
 \quad
 \begin{array}{c|ccccc}
 0 & 0 & 0 & 0 & 0 \\
 \frac{1}{2} & \frac{1}{2} & 0 & 0 & 0 \\
 \frac{1}{2} & 0 & \frac{1}{2} & 0 & 0 \\
 1 & 0 & 0 & 1 & 0 \\ \hline
 & \frac{1}{6} & \frac{1}{3} & \frac{1}{3} & \frac{1}{6}
 \end{array} \tag{1b}$$

Smooth analytical solution for coupling waves

- $\Omega^F := (0, 1) \times (0, 1)$, with $\rho^F := 1$, $\kappa := 1$, $c_p^F := 1$
- $\Omega^S := (-1, 0) \times (0, 1)$, with $\rho^S := 1$, $c_p^S := \sqrt{3}$, $c_s := 1$

Analytical solution is expressed in terms of u (acoustic) and $\mathbf{u} := (u_x, u_y)$ (elastic) so that

$$p := \partial_t u \quad \mathbf{m} := \nabla u \quad \text{in } \Omega^F, \quad (2a)$$

$$\mathbf{v} := \partial_t \mathbf{u} \quad \mathbb{C}^{-1} : \mathbf{s} := \nabla_{\text{sym}} \mathbf{u} \quad \text{in } \Omega^S. \quad (2b)$$

Source terms, (non)homogeneous Dirichlet boundary conditions, and initial conditions are defined according the following choices:

- Polynomial in space

$$u := (1 - x)x^2(1 - y)y \sin(\sqrt{2}\pi t) \quad u_x = u_y := (1 + x)x^2(1 - y)y \sin(\sqrt{2}\pi t); \quad (3a)$$

- Polynomial in time

$$u = u_x = u_y := x \sin(\pi x) \sin(\pi y) t^2. \quad (3b)$$

Ricker wavelet in academic test case

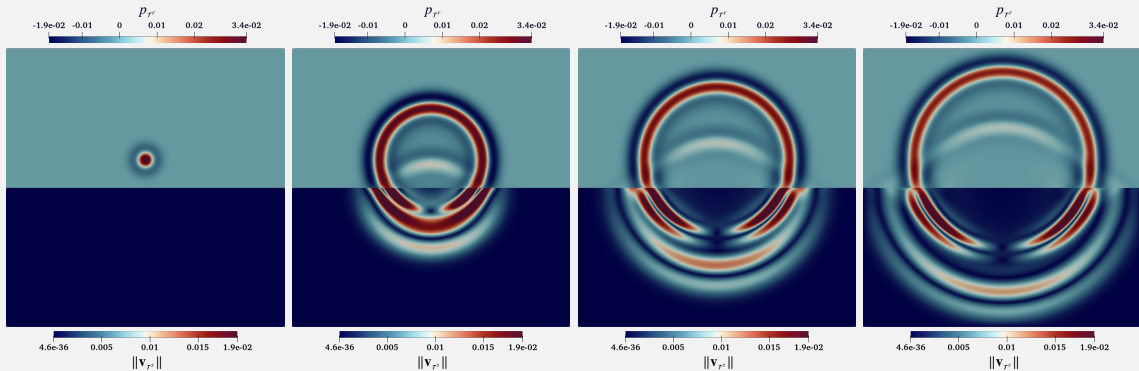


Figure 2: Spatial distribution of the acoustic pressure (upper side) and the elastic velocity norm (lower side) at times $t \in \{0, 0.25, 0.27, 0.32\}$ predicted by SDIRK(3, 4) scheme with mixed-order setting, $\mathcal{O}(\frac{1}{h})$ -stabilization, $k = 1$, $\ell = 7$, and $n = 9$.

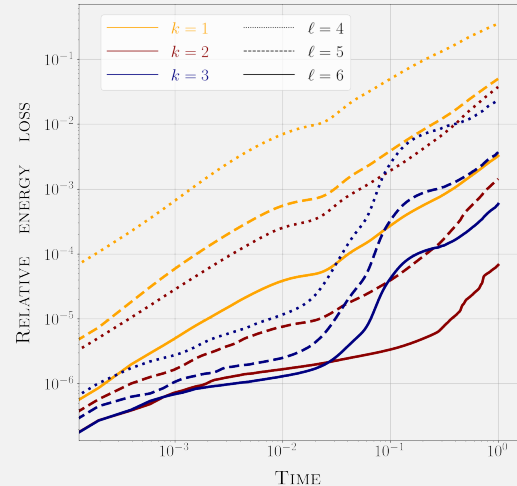
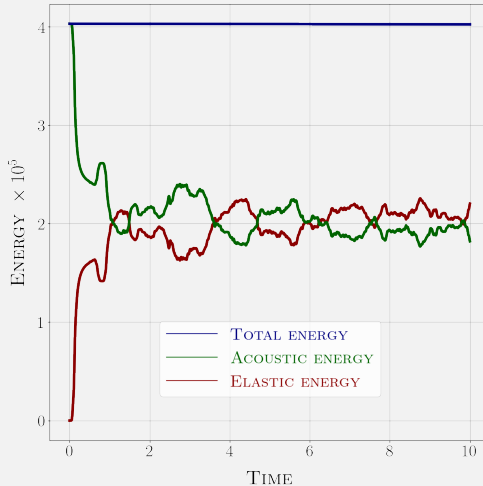


Figure 3: SDIRK(3,4) scheme with $n = 9$. **Left:** Energy repartition as a function of the time for $k = 3$ and $\ell = 6$. **Right:** Relative energy loss as function of the time for $k \in \{1, 2, 3\}$ and $\ell \in \{4, 5, 6\}$.

CFL stability limit

$$u(t, x, y) := x^2 \sin(\omega\pi x) \sin(\omega\pi y) \sin(\theta\pi t),$$

$$u_x(t, x, y) = u_y(t, x, y) := x^2 \cos(\omega\frac{\pi}{2}x) \sin(\omega\pi y) \cos(\theta\pi t),$$

- Dominant spatial evolution: $\omega := 5$ and $\theta := \sqrt{2}$
- Dominant temporal evolution: $\omega := 1$ and $\theta := 10$

Algorithm 1: Bounding of the CFL Stability Limit

```

1 while simulation is stable do
2   for n = 1 to N do
3     Compute energy  $E_n$ ;
4     Compute relative energy increase  $\Delta E := \max_n \left( \frac{|E_n - E_0|}{E_0}, \frac{|E_n - E_{n-1}|}{E_{n-1}} \right)$ ;
5     if  $\Delta E > \varepsilon$  then
6       Flag N as the first unstable time step;
7       break;
8   Flag N as the last stable time step;
9   Decrease N by  $\delta N$ ;

```

	$k = 1$			$k = 2$			$k = 3$		
	$s = 2$	$s = 3$	$s = 4$	$s = 2$	$s = 3$	$s = 4$	$s = 2$	$s = 3$	$s = 4$
CFL*	0.205	0.253	0.282	0.099	0.123	0.138	0.063	0.079	0.087
RATIO WRT s	1	1.23	1.38	1	1.24	1.39	1	1.25	1.38
RATIO WRT k	1	1	1	0.48	0.49	0.49	0.31	0.31	0.31

Table 3: CFL* coefficient (and ratios thereof) for ERK(s), $s \in \{2, 3, 4\}$ and $k \in \{1, 2, 3\}$.

MESHES	$s = 2$			$s = 3$			$s = 4$			
	\triangle	\square	\diamond	\triangle	\square	\diamond	\triangle	\square	\diamond	
$k = 1$	CFL*	0.191	0.205	0.264	0.238	0.253	0.329	0.265	0.282	0.363
	RATIO	1	1.07	1.38	1	1.06	1.38	1	1.06	1.37
$k = 2$	CFL*	0.106	0.099	0.136	0.133	0.123	0.170	0.147	0.138	0.188
	RATIO	1	0.93	1.28	1	0.92	1.28	1	0.94	1.28
$k = 3$	CFL*	0.072	0.063	0.082	0.090	0.079	0.102	0.100	0.087	0.115
	RATIO	1	0.88	1.13	1	0.88	1.13	1	0.87	1.15

Table 4: CFL* coefficient (and ratios thereof) for ERK(s), $s \in \{2, 3, 4\}$ and $k \in \{1, 2, 3\}$.

Efficiency study

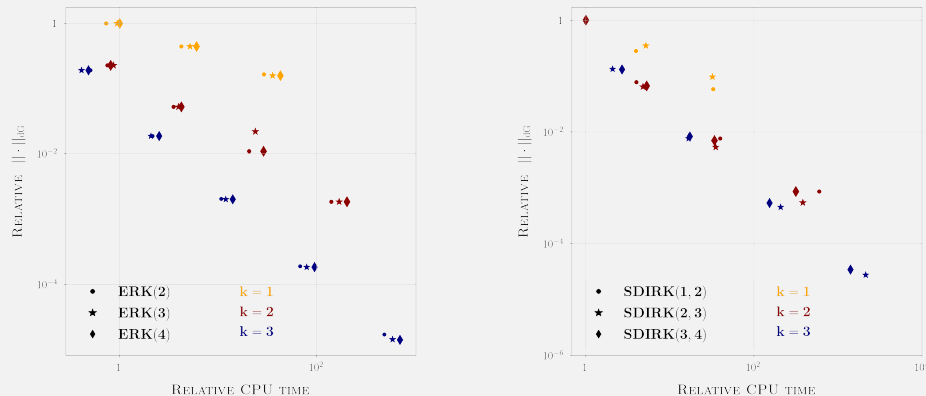


Figure 5: Test case with dominant spatial error. **Left panel:** Efficiency comparison for $\text{ERK}(s)$ for $s \in \{2, 3, 4\}$. **Right panel:** Efficiency for $\text{SDIRK}(s, s+1)$ for $s \in \{1, 2, 3\}$.

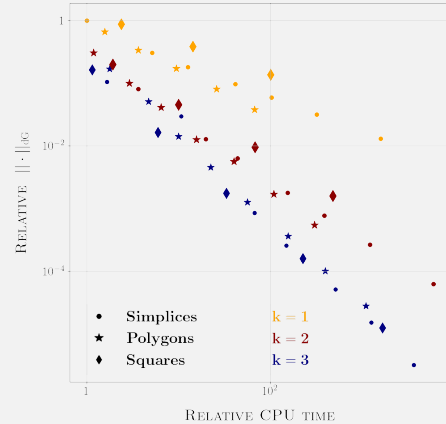
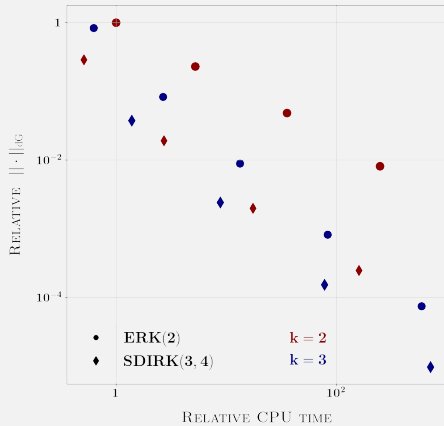


Figure 6: Test case with dominant spatial error. **Left panel:** Efficiency comparison for ERK(2) and SDIRK(3,4). **Right panel:** Efficiency comparison for ERK(4) on meshes composed of different cell geometries.

Coupling condition

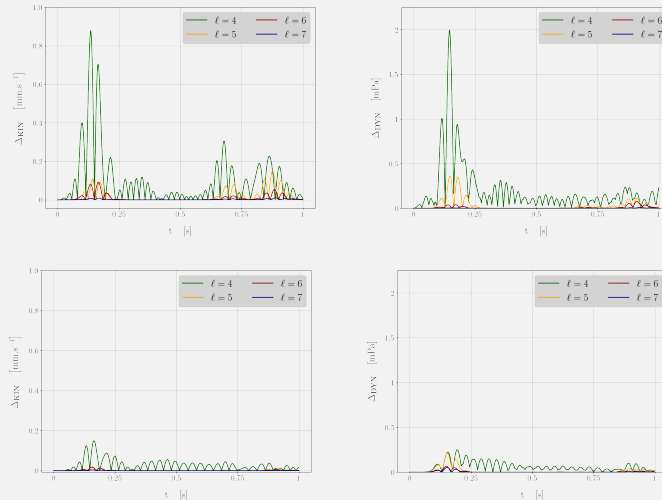


Figure 7: Errors on the coupling conditions as a function of the time predicted by SDIRK(3,4) for $k = 1$ (top row) and $k = 3$ (bottom row). **Left:** Kinematic errors. **Right:** Dynamic errors.

Efficiency study on Ricker wavelet

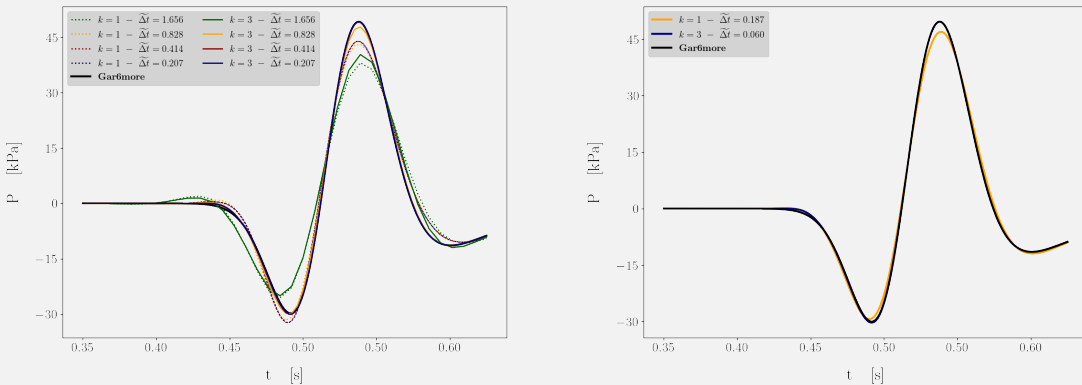


Figure 8: Spatial distribution of the acoustic pressure at \mathcal{S}^F at times $t \in [0, 0.625]$ [s]. **Left column:** SDIRK(3,4), $k \in \{1, 3\}$, and $\tilde{\Delta}t \in \{0.402, 0.805, 1.609, 3.219\}$. **Right column:** ERK(4), $k \in \{1, 3\}$ and $\tilde{\Delta}t = \{0.117, 0.363\}$ (recall that $CFL^* = 0.087$ for $k = 3$).

▲ What happen in ill-cut cells ?

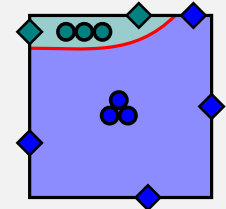
- Discrete trace inequality:

$$\|p_{T^i}\|_{(\partial T)^i} + \|p_{T^i}\|_{T^\Gamma} \lesssim C_{\text{TRACE}} h_T^{-\frac{1}{2}} \|p_{T^i}\|_{T^i},$$

- ▶ C_{TRACE} degenerate
- Stability and boundedness: For all $\hat{p}_T \in \hat{P}_T$,

$$|||\hat{p}_T|||^2 \lesssim a_T(\hat{p}_T, \hat{p}_T) \lesssim |||\hat{p}_T|||^2 := \|\nabla p_T\|_{T^i}^2 + h_T^{-1} \|p_T - p_{\partial T}\|_{(\partial T)^i}^2$$

- ▶ Not true anymore



■ Stabilization:

- ▶ Keep Lehrenfeld–Schöberl stabilization & Nitsche-like penalty at interface:

$$s_{\mathcal{M}}^{\circ}(\hat{p}_{\mathcal{M}}, \hat{q}_{\mathcal{M}}), \quad s_{\mathcal{M}}^{\Gamma}(\hat{p}_{\mathcal{M}}, \hat{q}_{\mathcal{M}})$$

- ▶ Ill-cut stabilization: Direct ghost penalty Preuß (2018) Lehrenfeld, Olshanskii (2019)

$$s_{\mathcal{M}}^{\mathcal{N}}(\hat{p}_{\mathcal{M}}, \hat{q}_{\mathcal{M}}) := \sum_{(T,i) \in \mathcal{P}_h^{\text{OK}}} \sum_{S \in \mathcal{N}_i^{-1}(T)} \frac{\kappa_i}{h_S^2} (\mathbf{p}_{S^i}^+ - \mathbf{p}_{T^i}, \mathbf{q}_{S^i}^+ - \mathbf{q}_{T^i})_{T^i}$$

- Connect ill-cut cell dofs with well-cut or uncut cell dofs

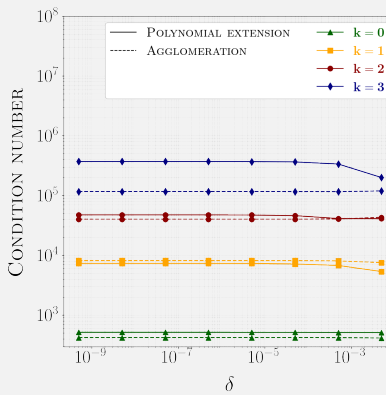
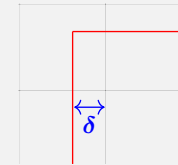
- ▶ Total stabilization:

$$s_{\mathcal{M}}(\hat{p}_{\mathcal{M}}, \hat{q}_{\mathcal{M}}) := s_{\mathcal{M}}^{\circ}(\hat{p}_{\mathcal{M}}, \hat{q}_{\mathcal{M}}) + s_{\mathcal{M}}^{\Gamma}(\hat{p}_{\mathcal{M}}, \hat{q}_{\mathcal{M}}) + s_{\mathcal{M}}^{\mathcal{N}}(\hat{p}_{\mathcal{M}}, \hat{q}_{\mathcal{M}})$$

Conditioning of stiffness matrix

- Square interface with distance to mesh:

$$\delta = 0.5 \times 10^{-p}, \quad p \in \{1, \dots, 9\}$$



- Grow of conditioning with polynomial degree
- **Robust conditioning** for severe ill-cut configurations

Pairing criteria

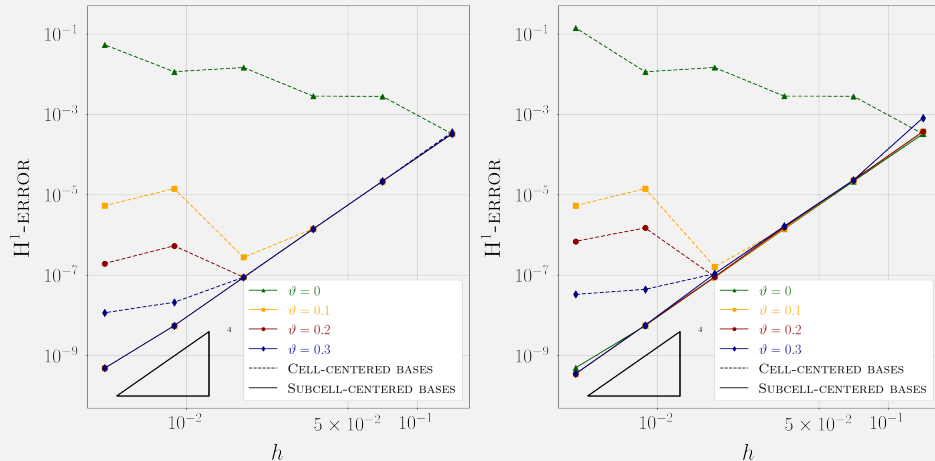


Figure 9: Errors as a function of the mesh size for the exact solution for $k = 3$ and various values of the pairing parameter ϑ used for flagging ill-cut cells. Left: polynomial extension. Right: cell agglomeration.

Convergence tests with high contrast property

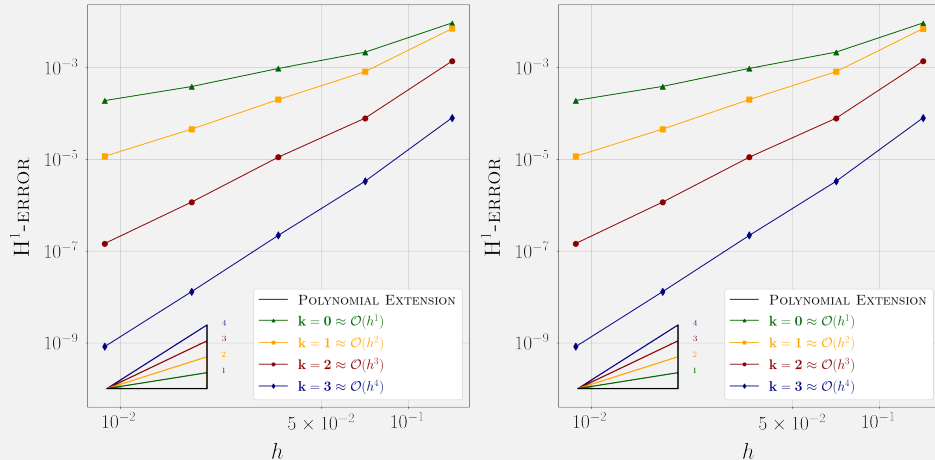


Figure 10: Errors as a function of the mesh size for the exact solution (left) and the exact solution (right) for various polynomial degrees $k \in \{0, \dots, 3\}$; diffusivity contrast set to $\kappa_2 = 10^4 \kappa_1$.

Convergence tests for non polynomial solution

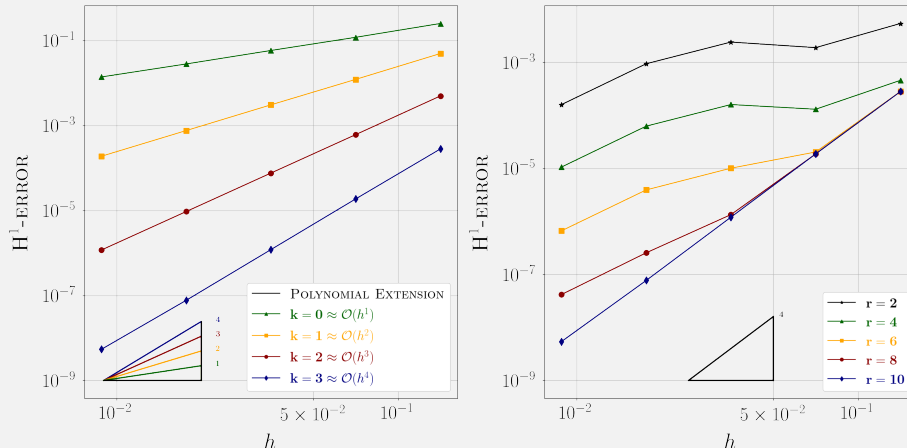


Figure 11: Left: Errors as a function of the mesh size for the exact solution for various polynomial degrees $k \in \{0, \dots, 3\}$ (with sub-triangulation parameter set to $r = 10$). Right: Errors as a function of the mesh size for $k = 3$ and $r \in \{2, 4, 6, 8, 10\}$. No diffusivity contrast.